PULSED-FOCUSING RECIRCULATING LINACS FOR MUON ACCELERATION

Final Report for Project starting 06/30/2008, ending 06/14/2012

Principal Investigator: Rolland Johnson

Small Business: Muons, Inc.
552 N. Batavia Ave.
Batavia, IL 60510

Muons, Inc. PI**:** Dr. Rolland Johnson

Research Institution: Thomas Jefferson National Accelerator Facility
12000 Jefferson Ave.
Newport News, VA 23606

Research Inst. PI: Dr. Alex Bogacz

2nd Research Inst.: Old Dominion University
Research Foundation, P.O.Box 6396
Norfolk, VA 23508-0369

ODU Principal: Dr. Vasiliy Morozov

Approved for public release; further dissemination unlimited. (Unclassified Unlimited)

PREPARED FOR THE UNITED STATES

DEPARTMENT OF ENERGY

Work Performed Under grant DE-FG02-08ER86351

DISCLAIMER

ABSTRACT

Since the muon has a short lifetime, fast acceleration is essential for high-energy applications such as muon colliders, Higgs factories, or neutrino factories. The best one can do is to make a linear accelerator with the highest possible accelerating gradient to make the accelerating time as short as possible. However, the cost of such a single linear accelerator is prohibitively large due to expensive power sources, cavities, tunnels, and related infrastructure. As was demonstrated in the Thomas Jefferson Accelerator Facility (Jefferson Lab) Continuous Electron Beam Accelerator Facility (CEBAF), an elegant solution to reduce cost is to use magnetic return arcs to recirculate the beam through the accelerating RF cavities many times, where they gain energy on each pass. In such a Recirculating Linear Accelerator (RLA), the magnetic focusing strength diminishes as the beam energy increases in a conventional linac that has constant strength quadrupoles. After some number of passes the focusing strength is insufficient to keep the beam from going unstable and being lost. In this project, the use of fast pulsed quadrupoles in the linac sections was considered for stronger focusing as a function of time to allow more successive passes of a muon beam in a recirculating linear accelerator. In one simulation, it was shown that the number of passes could be increased from 8 to 12 using pulsed magnet designs that have been developed and tested. This could reduce the cost of linac sections of a muon RLA by 8/12, where more improvement is still possible. The expense of a greater number of passes and corresponding number of return arcs was also addressed in this project by exploring the use of ramped or FFAG-style magnets in the return arcs. A better solution, invented in this project, is to use combined-function dipole-quadrupole magnets to simultaneously transport two beams of different energies through one magnet string to reduce costs of return arcs by almost a factor of two. A patent application was filed for this invention and a detailed report published in Physical Review Special Topics. A scaled model using an electron beam was developed and proposed to test the concept of a dog bone RLA with combined-function return arcs. The efforts supported by this grant were reported in a series of contributions to particle accelerator conferences that are reproduced in the appendices and summarized in the body of this report.

Table of Contents

Overview

Both Neutrino Factories (NF) and Muon Colliders (MC) require very rapid acceleration due to the short lifetime of muons. After a capture and bunching section, a linac raises the energy to about 900 MeV, and is followed by one or more Recirculating Linear Accelerators (RLA), possibly followed by a Rapid Cycling Synchrotron (RCS) or Fixed-Field Alternating Gradient (FFAG) ring. A RLA reuses the expensive RF linac sections for a number of passes at the price of having to deal with different energies within the same linac. Various techniques including pulsed focusing quadrupoles, beta frequency beating, and multipass arcs have been investigated via simulations to improve the performance and reduce the cost of such RLAs.

This project considered the design a single-linac RLA that incorporates pulsed focusing quadrupoles for use with ILC-type SRF accelerating structures at 1.3 GHz. Technical solutions for fast pulsed quadrupoles were investigated to determine feasibility and potential cost savings. The design included optics for the multi-pass linac and droplet-shaped return arcs where chromatic effects are assessed and appropriate compensation schemes designed.

There is no compatibility problem between the pulsed quadrupoles and the TESLA cavities from a magnetic standpoint. All the RLA pulsed quadrupoles must be placed outside of the cryomodules due to their magnetic fields and their heat load. Their fringe fields fall off very quickly with distance due to their small apertures. However, since the apertures of the quads are much smaller than that of the cavities, the question of wakefields must also be carefully considered.

Our study of RLAs based on the ILC linac with pulsed linac quads assumes a 90 degree phase advance/cell FODO optics configured with ILC-style cryomodules joined by normal-conducting quadrupole girders. We assume a conservative quad pulsing ramp rate of 1 Tesla pole field over 1 ms. Details of the quad ramping scheme are described in Appendix III.

Since the beam traverses the linac in both directions throughout the course of acceleration, one would like to maintain a 90° phase advance per cell for the lowest energy pass (the initial half-pass) by scaling the quad gradients with increasing energy along the linac. In order to mitigate the underfocus beta beating for the subsequent passes, the other half of the linac would have the inverted scaling of the quadrupole gradients – the so called 'bisected linac'. The resulting mirror symmetric focusing profile supports maximum number of passes in a 'dogbone' RLA as described in detail in Appendix I.

FODO lattice droplet arc design: includes the design of the separator region where the opposite muon charge species are steered in opposite directions around the arc. At the ends of the RLA linacs the beams need to be directed into the appropriate energy-dependent (pass-dependent) 'droplet' arc for recirculation. For practical reasons, horizontal beam separation was chosen. Rather than suppressing the horizontal dispersion

created by the spreader, the horizontal dispersion has been smoothly matched to that of the outward 60 deg. arc. Then, by an appropriate pattern of removed dipoles in three transition cells, the dispersion for the inward bending 300 deg. arc is flipped. The entire 'droplet' arc architecture is based on 90 degree phase advance cells with uniformly periodic Twiss functions.

Chromatic effects and compensation schemes have been addressed. Even with uniform multi-pass linac optics (bisected quad profile), considerable betatron matching is required between the linac and the droplet arcs. This involves a number of matching quads in the spreader-recombiner region of the droplet arc, which in turn 'breaks' the intrinsic cancellation of chromatic effects offered by the 90 degree phase advance/cell optics. For muon beams with momentum spread ~ 1%, this would still result in horizontal emittance dilution across the spreader/recombiner region. To mitigate that, one can use two families of sextupoles placed in the dispersive regions of spreader/recombiner. This scheme is very effective and completely eliminates emittance dilution.

Energy deposition from muon decay simulation and mitigation. For the cavities, the greatest difference between electrons and muons is that the latter decay. The energy deposited somewhere along the linac beamline by the decay electrons for the 30-2000 GeV, 16 pass Barbell with 2E11 muons will be about 27 mJ/m/cycle. This is too large to be ignored and too small to be a show-stopper. As the aperture of the pulsed quadrupoles will be smaller than that of the cavities, the quadrupoles provide a serendipitous collimator to absorb the decay electrons and positrons and their synchrotron radiation. This idea could be augmented by tungsten beam-pipe liners upstream and absorbers downstream of the pulsed quadrupoles. By these means a large fraction of the energy could end up in the warm rather than the cold components, and the deposition in the cold components would be spread over a larger volume.

The full accelerator complex for TeV energies is shown schematically in Fig. 1 below. After the pions are produced and the muons are collected, cooled and accelerated to 3 GeV, the first RLA is used to accelerate to 30 GeV where the muon bunches are coalesced. They are then accelerated in a second RLA to 750 GeV and injected into the collider ring.

To provide sufficient muon flux for either a MC or NF will require a high power proton driver over 4 MW of beam power at some energy greater than 6 GeV. Intense proton bunches are tightly focused onto a target capable of many MW operation [1] to produce an intense pion beam. The pions are captured in a strong solenoidal field where they decay into muons (and neutrinos). At the end a 40 m pion decay channel the muon beam has transverse normalized emittances of around 40,000 mm-mr and is spread in time over tens of ns. The transverse dimensions of the beam must be cooled to be small enough and bunches must formed to fit into reasonable accelerating structures. For a MC, this is about a factor of a thousand in each transverse plane, or a factor of a million in six-dimensional emittance reduction.

The first RLA proper goes from about 3 to 30 GeV. The goal is to increase the number of passes through the linac in a RLA in order to reduce the cost. Our new bisected optics, in

which the quadrupole strengths increase with distance to the center of the linac, allows an increase in the number of passes via beta function beating, while ramping up the quadrupoles in time (pulsing them) further increases the number of passes. The muons large emittance limits the number of arcs at each end to be about 3, so the advantage of multiple passes through the linac is limited by the return arcs.

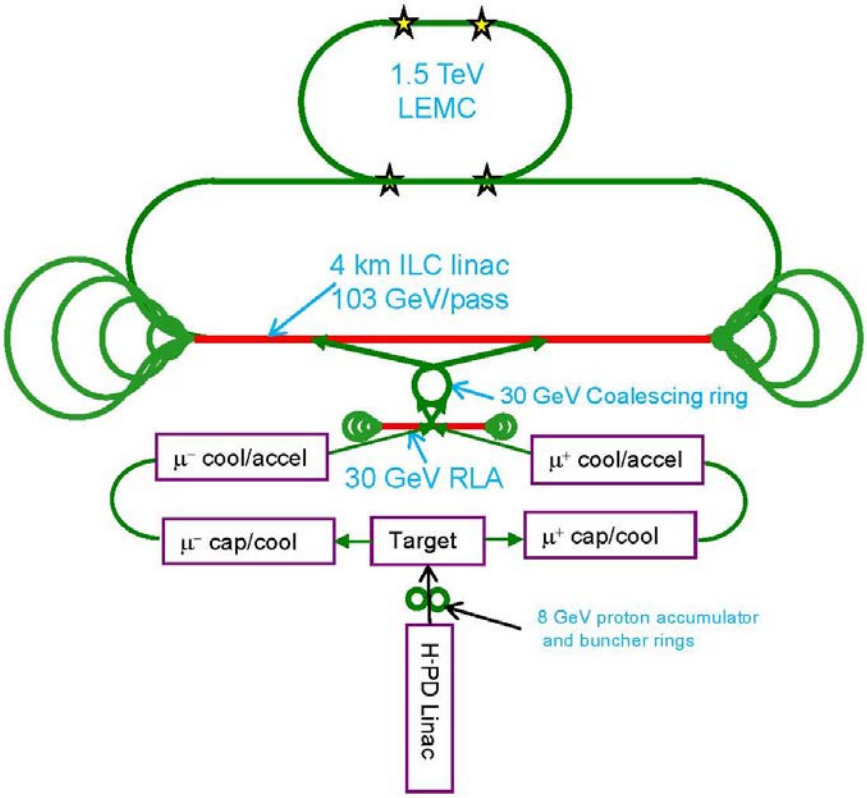

Figure 1: Conceptual diagram of a high energy muon collider with dog bone RLAs using multipass teardrop return arcs to minimize the costs of acceleration. Five km of RF structures accelerate both signs of muon for 1.5 TeV COM collisions on a small footprint that easily fits on the Fermilab site. The ILC requires over 30 km of RF structures to achieve 0.5 TeV COM e+e- collisions.

Three Gev linear pre-accelerator

A single-pass linac "pre-accelerator" raises the beam energy to 3 GeV. This makes the muons sufficiently relativistic to facilitate further acceleration in an RLA. In addition, the longitudinal phase space volume is adiabatically compressed in the course of acceleration [2]. The large acceptance of the pre-accelerator requires large aperture and tight focusing at its front-end. Given the large aperture, tight space constraints, moderate beam energies, and the necessity of strong focusing in both planes, we have chosen solenoidal focusing for the entire linac [3]. To achieve a manageable beam size in the linac front-end, short focusing cells are used for the first 12 cryo-modules. The beam size is adiabatically damped with acceleration, and that allows the short cryo-modules to be replaced with the intermediate length cryomodules, and then with 22 long cryomodules as illustrated in Fig. 2.

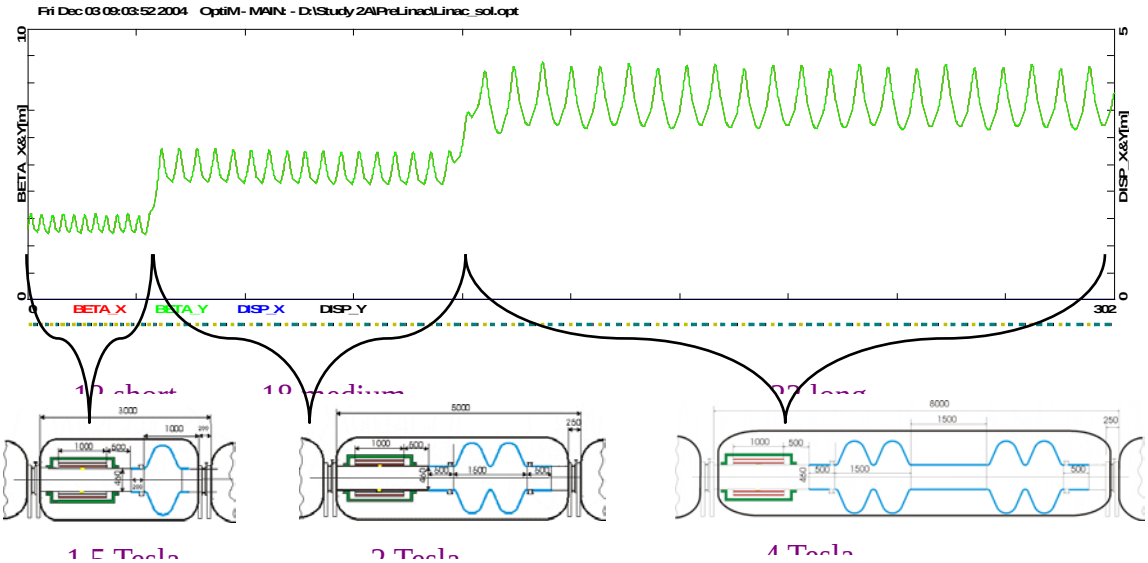

Figure 2: Transverse optics – uniform periodic focusing with 12 short, 18 medium, and 22 long cryo-modules.

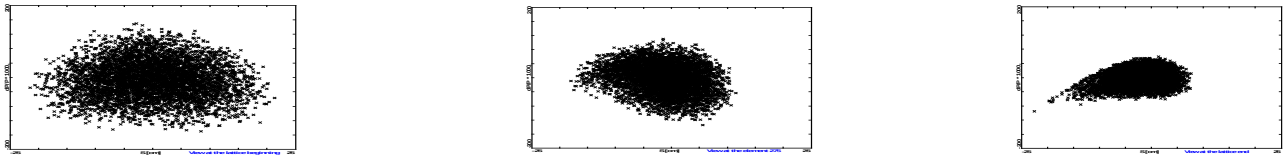

Figure 3: Particle tracking results showing adiabatic bunch compression along the linac. The longitudinal phase-space (z, Δp/p) is shown at the linac entrance, at the middle and at the linac end. Particle marked in green are lost during tracking (outside the 20 cm aperture).

The initial longitudinal acceptance of the linac is chosen to be 2.5σ, i.e. $\Delta p/p = \pm 17\%$ and RF pulse length $\Delta\phi = \pm 72º$. To perform adiabatic bunching [2,3], the RF phase of the cavities is shifted by 72º at the beginning of the pre-accelerator and then gradually changed to zero by the end of the linac. In the first half of the linac, when the beam is still not completely relativistic, the offset causes synchrotron motion which allows bunch compression in both length and momentum spread, yielding $\Delta p/p = \pm 7\%$ and $\Delta\phi = \pm 29º$. The synchrotron motion also suppresses the sag in acceleration for the bunch head and tail. In our tracking simulation we have assumed a particle distribution that is Gaussian in 6D phase space with the tails of the distribution truncated at 2.5σ, which corresponds to the beam acceptance. Despite the large initial energy spread, the particle tracking simulation through the linac does not predict any significant emittance growth. There is a 0.4% beam loss coming mainly from particles at the longitudinal phase space boundary. Results of the simulation are illustrated in Fig. 3, which shows 'snapshots' of the longitudinal phase space at the beginning and at the end of the Pre-accelerator.

Multi-pass linac optics

The superconducting accelerating structure is by far the most expensive component of the accelerator complex. Maximizing the number of passes in the RLA can significant lower the cost [4] of the overall acceleration scheme.

There are two notable advantages of the 'Dogbone' configuration compared to the 'Racetrack' (such as CEBAF)

- Better orbit separation at the linac ends resulting from larger (factor of two) energy difference between two consecutive linac passes.
- Favorable optics solution for simultaneous acceleration of both μ± species can be supported by the 'Dogbone topology', which allows both charge species to traverse the RLA linac in the same direction while passing in the opposite directions through the mirror symmetric optics of the return 'droplet' Arcs.

The key element of the transverse beam dynamics in a 'Dogbone' RLA is an appropriate choice of multi-pass linac optics [5]. The focusing profile along the linac (quadrupole gradients) need to be set so that one can transport (provide adequate transverse focusing for given aperture) multiple pass beams within a vast energy range. Obviously, one would like to optimize the focusing profile to accommodate maximum number of passes through the RLA. The RLA layout illustrated in Figure 4, features a 'Dogbone' based on a 500 meter long (20 FODO cells with 8 RF cavities/cell) 4 GeV linac with the injection energy of 3 GeV. The alternative structure is called a racetrack, where the CEBAF machine at Jefferson Lab is an example.

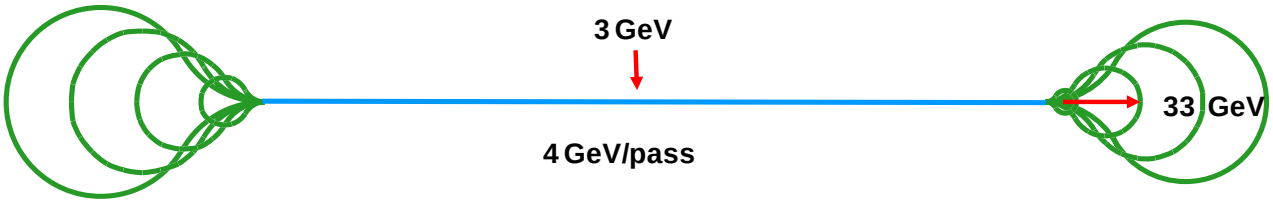

Figure 4: The RLA layout features a 'Dogbone' based on a 250 meter long linac (20 FODO; 4 RF cavities/cell).

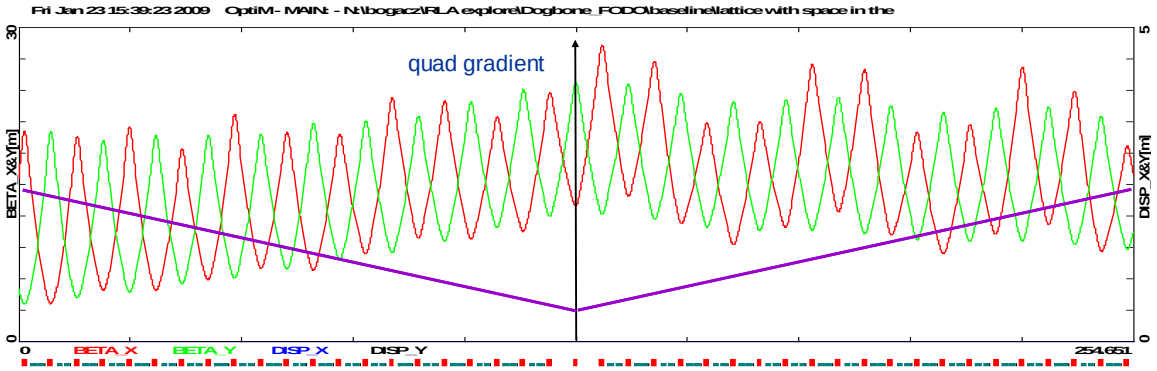

Figure 5: Bisected linac Optics – mirror symmetric quadrupole gradient profile minimizing under-focus beta beating.

Since the beam is traversing the linac in both directions throughout the course of acceleration, one would like to maintain a 90° phase advance per cell for the lowest energy pass (the initial half-pass) by scaling the quad gradients with increasing energy along the linac. In order to mitigate the beta beating due to reduced focusing for the subsequent passes, the other half of the linac would have the inverted scaling of the quadrupole gradients. The resulting mirror symmetric focusing profile of the linac is illustrated in Fig. 5.

Now we consider a 'Pulsed' linac Optics for the same RLA layout. Here we assume a time varying quad strength in the RLA linac described in the previous section. A feasible quad pulse would assume a 500 Hz cycle ramp with the top pole field of 1 Tesla. That would translate to a maximum quad gradient of G^{max} =2 kG/cm (5 cm bore radius) ramped over τ = 1 ms from the initial gradient of G_0 =0.1 kG/cm. We have used a fairly conservative rise time based on similar applications for ramping the new corrector magnets for the Fermilab Booster that have 1 kHz capability [4].

For simplicity, we consider a linear ramp according to the following formula:

$$G(t) = G_0 + \frac{G^{\max} - G_0}{\tau} t \tag{1}$$

A single bunch travelling with a speed of light along the linac with quads ramped according to Eq.(1), 'sees' the following quad gradient passing through the i-th cell along the linac (I = 1,…20)

$$G_i = G_0 + \frac{G^{\max} - G_0}{\tau} \frac{\ell_{cell}}{c} i \tag{2}$$

where ℓ_{cell} is the cell length and i defines the bunch position along the linac.

For multiple passes through the linac (the index n defines the pass number) the above formula can be generalized as follows:

$$G_i^n = G_0 + \frac{G^{\max} - G_0}{\tau c} \left[(n-1) \left(\ell_{linac} + \frac{n}{2} \ell_{arc} \right) + i \ell_{cell} \right] \tag{3}$$

where ℓ_{linac} is the full linac length and ℓ_{arc} is the length of the lowest energy droplet arc. Here we also assume that the energy gain per linac is much larger than the injection energy. Fig. 6 illustrates the multi pass optics for the pulsed linacs. As one can see below, there is sufficient phase advance to support up to 12 passes.

Pass 8 (31-35 GeV)

Fixed

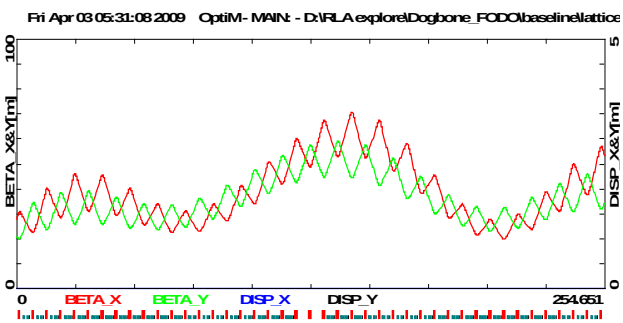

Pulsed

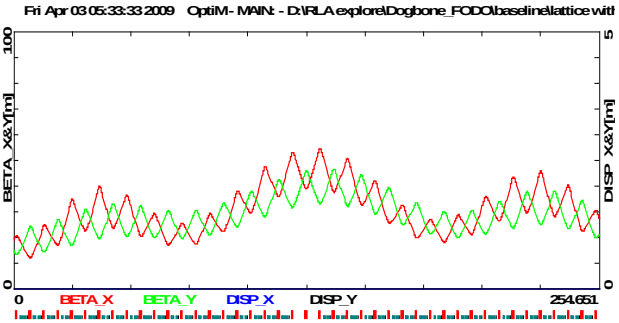

Pass 12 (47-51 GeV)

Fixed

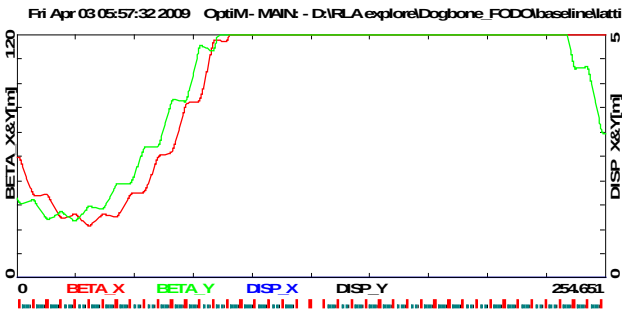

Pulsed

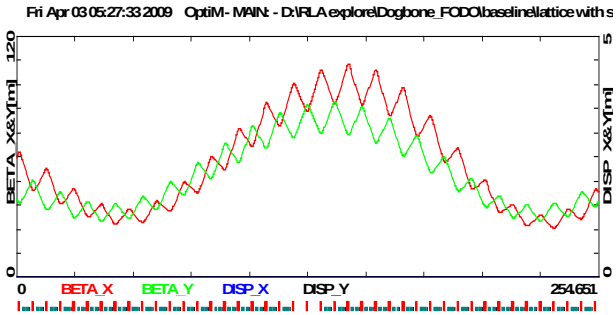

Figure 6: The 8-th pass and the last one (12-th) of the pulsed linac optics. By pulsing the focusing quads as described in Eq.(3), the additional 4 passes increase the output energy from 35 to 51 GeV. Red is horizontal and green is vertical.

Ramped Quad Magnets

The issue of rapidly ramped magnets has been studied previously and the values reported here are based on that work [6]. Assuming the muons have normalized emittances of ~40 mm-mr and beta functions ~20 m, at 3 GeV the largest aperture needs to be

$$10\,\sigma_{\perp} = 10\sqrt{\frac{\sigma_{\perp}^{N}\,\beta_{\perp}}{\beta\gamma}} \sim 53 \text{ mm} \qquad (4)$$

The energy stored in the yokes is small with respect to that in the vacuum since the energy density goes as 1/μ, so with a 1m quadrupole of gradient ~1 T/m the stored energy is only

$$W = \frac{1}{2\mu}\int B^2 dV \sim 3 \text{ J/m} \qquad (5)$$

The stored energy increases by the square of the gradient, so at 33 GeV the stored energy would be ~380 J/m, requiring ~400 kW/m driving power. Roughly similar magnets are already in use [7].

Droplet Arcs

In a 'Dogbone' RLA one needs to separate different energy beams coming out of a linac and to direct them into appropriate 'droplet' arcs for recirculation [2]. For multiple practical reasons, horizontal rather than vertical beam separation was chosen. Rather than suppressing horizontal dispersion created by the Spreader, it is smoothly matched to the horizontal dispersion of the outward 60^0 arc. Then by the appropriate pattern of removed dipoles in three transition cells, one 'flips' the dispersion for the inward bending 300^0 arc, etc. The entire 'droplet' Arc optics architecture is based on 90^0 betatron phase advance cells with uniform periodicity of Twiss functions. The resulting 'droplet' Arc optics based on FODO focusing [3] is illustrated along with its 'footprint' in Figure 7.

Arc 1

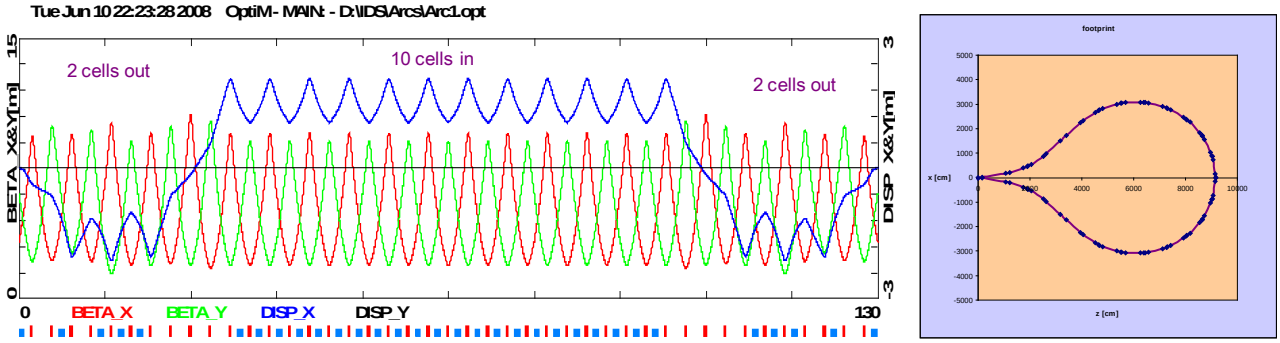

Arc 4

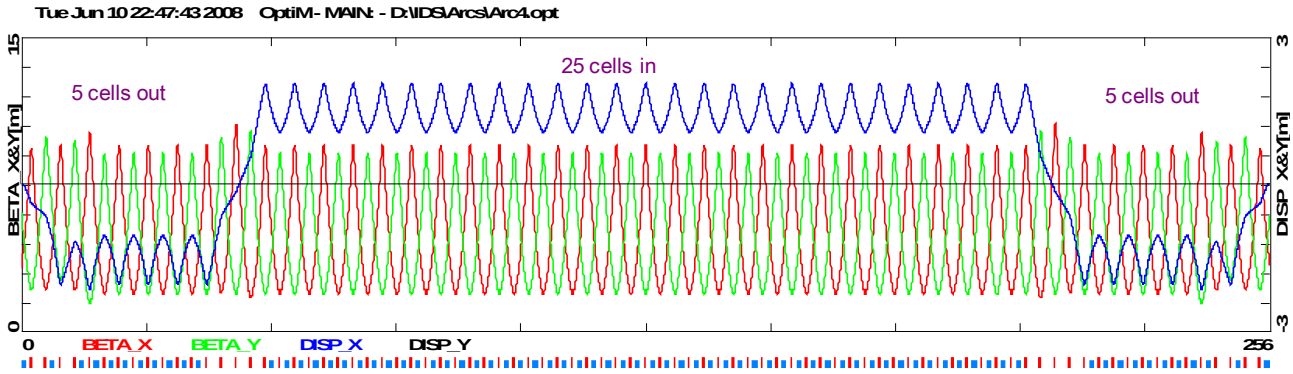

Figure 7: 'Droplet' Arc optics and its 'footprint' – uniform periodicity of beta functions and dispersion. The design offers both compactness and modularity; the top plot illustrates the lowest energy arc. The higher arcs based on the same bending field are configured by adding periodic cells in the outward and inward bending sections, extending the circumference and increasing the quadrupole strength according to the momentum. The bottom plot illustrates Arc 4.

High Energy RLA

An RLA for a high energy MC (much greater than 30 GeV) is different from one intended only for a NF. The survival of the muons is essentially dependent just on the average accelerating gradient over the entire path. The arc magnets represent a very large part of the path. It quickly becomes impractical to build single-pass or even NS-FFAG arcs, and one can consider pulsed (also called fast ramped) arc magnets. This ramping and the size of the arcs precludes any possibility of using the same magnets for both polarity muons travelling in opposite directions To limit the size of the arcs, strong static superconducting dipoles are needed, while to ramp up the field quickly enough fast normal conducting dipoles are needed used too, leading to a hybrid design.[8] Such a hybrid is limited by the strength of the dipoles and the momentum range it need span, but could have a dual bore design to accommodate muons of both signs to reduce cost. Such large RLAs begin to resemble a Rapid Cycling Synchrotron (RCS); the final choice of dogbone, racetrack or circle becomes a question of cost. A much better solution for high and lower energy RLAs is described next.

Multi-pass arcs using combined function dipole-quadrupole magnets

Using pulsed quad focusing profile in the linac increased number of passes from 8 passes to 12 leading to cost savings. However, in that scheme, one needs to separate different energy beams coming out of a linac and to direct them into appropriate droplet-shaped arcs for recirculation. Each pass through the linac would call for a separate fixed energy droplet arc, increasing the complexity of the RLA.

We first considered ramped and Fixed Field Alternating Gradient (FFAG) droplet arcs. Arcs using ramped or pulsed magnets are limited by the speed of the ramping and their maximum field and cannot accommodate simultaneous passes of $\mu+$ and $\mu-$ traveling in opposite directions. FFAG arcs accept multiple momenta at a given field and can simultaneously accommodate $\mu+$ and $\mu-$ traveling in opposite directions. However, FFAG arcs have dipoles with reverse bends, which makes them longer and more expensive.

However, an even more attractive solution is the use of combined-function magnets that allow two or even three passes of muons in one droplet arc. This invention is described in appendix VI and a corresponding patent application [9]. A complete description of the work was published in PRSTAB [10], which is reproduced in Appendix IX.

A dogbone RLA model with combined-function magnet recirculating arcs was proposed to experimentally verify the concepts developed in this project with a scaled model using electrons instead of muons. This concept was developed and proposed as described in appendix VII as a possible straightforward test by scaling a GeV scale muon design. Scaling muon momenta by the muon-to-electron mass ratio leads to a scheme, in which a 4.5 MeV electron beam is injected at the middle of a 3 MeV/pass linac with two double-pass return arcs and is accelerated to 18 MeV in 4.5 passes. All spatial dimensions including the orbit distortion are scaled by a factor of 7.5, which arises from scaling the 200 MHz muon RF to the frequency readily available at CEBAF: 1.5 GHz. The footprint of a complete RLA fits in an area of 25 by 7 m. The scheme utilizes only fixed magnetic fields including injection and extraction. The hardware requirements are not very demanding, making it straightforward to implement.

CONCLUSIONS

Intense muon beams for Muon Colliders, Neutrino Factories, and other physics and commercial ventures demand extensive use of linac technologies for their production, cooling, capture, beam formation/shaping and acceleration. The short muon lifetime and large emittance when they are created drives the technology. Recirculating Linear Accelerators (RLAs) can provide exceptionally fast and economical muon acceleration. They are limited to the extent that the focusing range of the RLA quadrupoles allows each muon to pass several times through each high-gradient cavity and by the return arcs. The new concepts of rapidly changing the strength of the RLA focusing quadrupoles and use beta function beating as the muons gain energy has been developed that significantly increases the number of passes that each muon will make in the RF cavities, while the ideas of rapidly ramping the arc magnets and the use of NS-FFAG magnets reduces the cost and complexity of the return arcs. A droplet arc design based on combined-function magnets has been developed to transport muon beams of two passes for both charge species. This lowers the number of arcs and eases the design of a muon RLA. A complete linear lattice for the 3 to 33 GeV RLA has been designed (multi pass-linac with pulsed quads and 12 droplet arcs). A scale-model test of the dog bone RLA with combined function magnets using an electron beam has been proposed. Such a demonstration would lead to more confidence that the numerical simulations are correct and that there is a path for affordable acceleration of high-energy muon for neutrino factories and muon colliders.

REFERENCES

[1] H. G. Kirk, H. Park, T. Tsang, J. R.J. Bennett, O. Caretta, P. Loveridge, A. J. Carroll, V. B. Graves, P. T. Spampinato, I. Efthymiopoulos, A. Fabich, F. Haug, J. Lettry, M. Palm, H. Pereira, K. T. McDonald, N. V. Mokhov, S. I. Striganov, The MERIT High-power Target Experiment at the CERN PS. http://accelconf.web.cern.ch/AccelConf/e08/papers/wepp169.pdf

[2] S.A. Bogacz, Nuclear Physics B, Vol 155, 334, (2006)

[3] J.S. Berg et al., Physical Review Special Topics Accelerators & Beams, 9, 011001 (2006)

[4] V.S. Kashikhin et al., PAC05

[5] G.M. Wang, K.B. Beard, R.P. Johnson, S.A. Bogacz, Pulsed Magnet Arc Designs for Recirculating Linac Muon Accelerators. http://accelconf.web.cern.ch/AccelConf/PAC2009/papers/we6pfp097.pdf

[6] G.M. Wang, S.A. Bogacz, R.P. Johnson, D. Trbojevic, Multipass Arc Lattice Design for Recirculating Linac Muon Accelerators, http://accelconf.web.cern.ch/AccelConf/PAC2009/papers/we6pfp098.pdf

[7] D. J. Summers, L. M. Cremaldi, T. L. Hart, L. P. Perera, M. Reep (1), H. Witte (2), S. Hansen, M. L. Lopes (3), J. Reidy, Jr. Test of a 1.8 Tesla, 400 Hz Dipole for a Muon Synchrotron, arXiv:1207.6730v1 [physics.acc-ph]

[8] Hybrid Arc design ref.

[9] http://www.google.com/patents/WO2013043833A1?cl=en

[10] V. S. Morozov, S. A. Bogacz, Y. R. Roblin, and K. B. Beard, Linear fixed-field multipass arcs for recirculating linear accelerators, PHYSICAL REVIEW SPECIAL TOPICS - ACCELERATORS AND BEAMS 15, 060101 (2012) http://journals.aps.org/prstab/pdf/10.1103/PhysRevSTAB.15.060101

PULSED MAGNET ARC DESIGNS FOR RECIRCULATING LINAC MUON ACCELERATORS*

K.B. Beard#, R.P. Johnson, Muons, Inc. Batavia, IL USA
S.A. Bogacz, JLab, Newport News, VA USA
G.M.Wang, Muons, Inc., Batavia IL, and Old Dominion University, Norfolk, VA, USA

Abstract

Recirculating linear accelerators (RLAs) using both pulsed quadrupoles and pulsed dipoles can be used to quickly accelerate muons in the 3 – 2000 GeV range. Estimates on the requirements for the pulsed quadrupoles and dipoles are presented.

RAMPED MAGNET LIMITATIONS

For a single return arc of a muon RLA, the radius is determined by the momentum and the magnetic dipole field averaged over the arc:

$$R_{arc} = P_{max}/(300\text{MeV/T-m})/B_{avg}$$

It is not feasible to ramp superconducting magnets fast enough to accelerate short-lived muons [8]; only magnets that are normally conducting might ramp fast enough. In a hybrid cell consisting of normal and superconducting magnets, the normally conducting magnets fields can swing from –Bn to +Bn while the field Bs in the superconducting magnets remains constant. The largest average field is determined by a combination of the limits on Bs and Bn, the fraction of the cell filled with dipoles f, and the ratio of final to initial energy.

$$P_{max}/P_{min} = B_{max}/B_{min} = (Bs\cdot Ls + Bn\cdot Ln)/(Bs\cdot Ls - Bn\cdot Ln)$$

$$x \equiv (P_{max}/P_{min} - 1)/(P_{max}/P_{min} + 1)$$

$$B_{avg} = f\ Bs\ (x+1)/(x(Bs/Bn)+1)$$

Given the current state-of-the art, approximately Bs=8.8 T, Bn=1.8 T and f=1, so as $P_{max}/P_{min}\rightarrow\infty$, $B_{avg}\rightarrow 3.0$ T and for 2 TeV, R_{arc}=2.2 km and L_{arc}=16.3 km.

3-30 GEV CONCEPT

For lower energies, it is not necessary to consider the complexities of ramped magnets at all; Bogacz et al. [1] have shown that a bisected linac could accommodate up to 7 passes, while Wang et al [2] have shown that that linac with arcs based on a NS-FFAG lattice could accommodate multiple passes through a single arc.

A simple 3-30 GeV dogbone has one small superconducting single pass arc and a much larger, multiple pass NS-FFAG arc at each end with the beam injected in the middle of the linac going to the right.

Adding pulsed quadrupoles to the linac and another pair of NS-FFAG arcs to the ends increases the number of passes to 12 and the energy to 50 GeV [2]. Ramping the NS-FFAG arcs themselves is far less advantageous, as the increased path length due to the relatively low B_{avg} (~1/3 B_{max}) bending field of a NS-FFAG leads to excessive loss of the muons by decay.

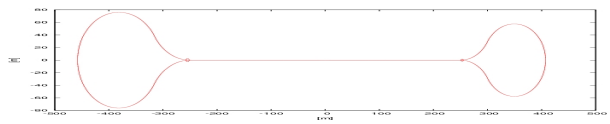

Figure 1: Conceptual design of a "dogbone" RLA for muon acceleration.

30-2000 GEV CONCEPT

As the ratio of maximum to minimum energy increases, the proliferation of arcs leaves little alternative to ramping the magnets. The basic concept of the barbell RLA is to inject the muons of both signs into an end of the linac going in the same direction.

Since the momentum of the muons does not change while in an arc, there would be a mismatch between the momentum and the local field if the same ramping magnet apertures were used for muons of both polarities.

This problem can be avoided by using either two sets of magnets or very large acceptance NS-FFAG magnets. The latter option increases the radius and hence the muon decay loss unacceptably.

Here, droplet-shaped return arcs are used. Each teardrop arc bends outward 60º, then inward 300º, then outward 60º again for a 180º turn, for a total circumference of (420º/360º)2πR. The optics advantages of droplet arcs are described elsewhere [1].

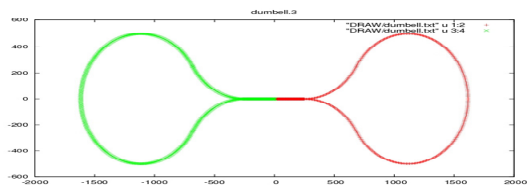

Figure 2: Conceptual design of a "barbell" RLA for muon acceleration.

The survival of muons through acceleration is determined by just the mean gradient over the whole acceleration path.

$$N/No \approx (E_i/E_f)^{(\lambda\mu\ m\mu)/(g\text{Linac c})\cdot(1+\text{Larc/Llinac})}$$

$$\approx (N/No_{\text{straight-linac}})^{(1+\text{Larc/Llinac})}$$

The design of the accelerator is a compromise among many variables, the most important being the gradient and length of the linac and the average magnetic field B_{avg} of the arcs. The details of the arcs become relatively less

*Supported in part by US DOE-STTR Grant DE-FG02-08ER86351 and JSA DOE Contract No. DE-AC05-06OR23177
beard@muonsinc.com

important as the linac gradient increases. An ILC-like 1.3GHz superconducting linac may provide as much as ~30 MeV/m of real estate gradient (including drifts, quadrupoles, etc.) averaged over the length of the linac.

As a starting point, consider a 4 km linac with 123 GeV/pass (30.8 MV/m). Using two identical teardrop arcs of radius 2.2 km and B_{avg}=3.0 T, only 1 msec and 16 passes would be required to reach full energy and 90% of the muons survive.

The normal magnets, though, would need to ramp from -1.8 to 1.8 T in one msec, for a rate of 3700 T/s. A similar barbell using only normal magnets in the arc would have a radius of 3.7 km, require 1.7 msec to ramp, and have only 84% of the muons survive.

RAMPED ARC MAGNETS

D.J. Summers et al. have considered the issues concerning rapidly ramping magnets for some time and in depth and these estimates in this paper are all heavily based on that work.[3][7][11]

Since the energy stored in a magnetic field volume goes as 1/μ, the energy stored in the iron is small compared with that stored in the vacuum.

For the proposed Low Emittance Muon Collider, the emittances of the muon beams are small, so the apertures may also be small. Assuming the muons have normalized emittances of 2.1 mm-mrad, beta functions < 20 m, at 30+123=153 GeV the aperture needs to be

$$10\,\sigma_{\perp} = 10\sqrt{[(\varepsilon_{\perp N}/\beta\gamma)\,\beta_y]} = 1.7 \text{ mm}.$$

To begin, consider an arc made only of normal magnets (B_{avg}≈1.8 T); the stored energy in the dipoles is

$$W = 1/(2\mu)\int B^2\,dV = \tfrac{1}{2}\,L\,I^2 = 3.7 \text{ J/m}$$

$$dW/dt = 2.2 \text{ kW}$$

The current through the magnet depends on the number of turns N_{turns} (here taken to be 1):

$$I = B\,h\,/\,\mu_o\,N_{turns} = 2400 \text{ A}$$

$$L = 2W/I^2 = 1.3\ \mu\text{H}$$

$$V = -L\,dI/dt = 4.5 \text{ kV}$$

This voltage is under the limitof 5 kV recommended by Ken Bourkland [11]. The arcs here are 27.15 km long (the circumference of the LHC!), so each requires 60 MW of ramp power. That leads to the suggestion that a resonant circuit could be considered. Roughly, the frequency ought to be ~150 Hz (4x the ramp time), so for a simple LC circuit:

$$C = 1/(2\,\pi\,L\,f^2) = 5.4 \text{ F/m}$$

A 3rd order component would probably need be superimposed to maintain a more linear ramp to match the energy gain of the linac; alternatively, the phasing of the linac could be modified during the ramp to make the energy gain match the magnets at some sacrifice in muon survival.

Using a laminated dipole design very similar to that proposed by D.J.Summers[7], the core losses for 12 mil 3% silicon steel can be described as [9]:

$$\text{Watts/kg} = 1.49\text{E-}3 \cdot f^{1.55}\,B^{1.71} \sim 10 \text{ W/kg}.$$

Assuming the magnet is about 2"x1.5" overall gives about 13kg/m of steel, or about 130 W/m from core losses. Ohmic heating of the copper conductors is about 800 W/m.

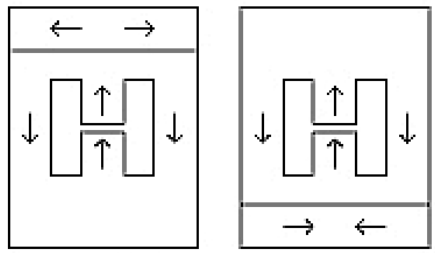

Figure 3: Alternating layers of a laminated normal ramped arc dipole magnet [7].

It is reasonable to have the two normal conducting magnets share the return yoke as in the LHC, reducing the size and cost of the two arcs. If the muons travel the same direction around the arc, the fields are equal and opposite.

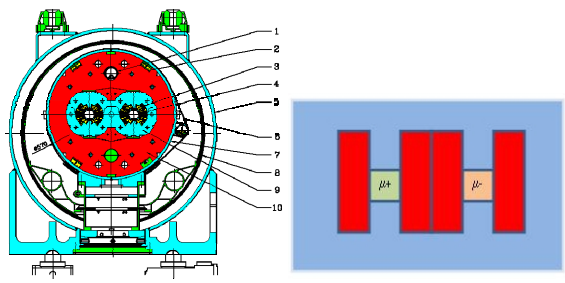

Figure 4: LHC shared yoke dipole schematic [10] and a cartoon of a dual warm ramped dipole.

A hybrid normal/superconducting magnet allows a higher average magnetic field; however, the rapidly changing field from the normal magnets must not penetrate the superconducting magnets. Due to the very small apertures, however, the required gaps have little impact on the overall length of the cell. The range of the momentum of the beams determines the maximum average field that can be made by the hybrid.

In this case, it may become advantageous to divide the momentum range between two arcs. Any advantage is greatly reduced as the energy/pass of the linac is increased.

For the hybrid case with a single arc at each end, B_{avg}=3 T, so the total ramp time is about 1 ms. The normal magnets swing from – to + 1.8 T, so the frequency is about 500 Hz, and the superconducting magnets remain unchanged. While the stored energy in the normal magnets is the same as before, the ramping power and voltages are about 3.3x as high and the core losses are about 6.5x as high. The cell length is dominated by the normal dipole (Ln=4.74 Ls), so averaging over the whole arc the power/length by is only decreased ~17%.

RAMPED QUAD MAGNETS

Both the linac and a single arc in a barbell will require very similar ramped quadrupole magnets.

At 30 GeV, the aperture needs to be also ~3 mm and the gradient ~10T/m for a 1 m quadrupole, while for 2000 GeV the aperture only needs to be ~0.5 mm and the gradient needs to be about ~300 T/m. Again the energy stored in the yokes is small with respect to that in the vacuum since the energy density goes as 1/μ.

As the beam energy is increased for a given beta function, the required aperture decreases and the gradient increases such that the stored energy would remain about the same, corresponding to about 0.2 J/m of stored energy. However, since the quadrupoles can't change aperture as the energy increases, the stored energy increases by the square of the gradient. By 2 TeV, the stored energy is 1.5 J/m and the power 1.5 kW. With 3% silicon steel return yoke, the core losses would be only ~ 80W/m at 2000 GeV.

As in the case of the dipoles, a resonant circuit to move the energy in and out of the field is a possibility.

It ought to be noted that while the arc quadrupole gradients do scale with the average B·dl of a cell, they do not scale with the normal components of a hybrid cell, making a combination design problematic.

The Fermilab Booster is upgrading to ramped combination corrector magnets as shown in Figure 5 [4]. These have about ~6x the stored energy/length of RLA quadrupoles and can switch full quadrupole field polarity in 1 ms.

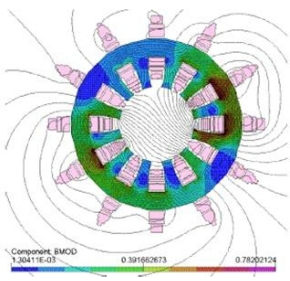

Figure 5: FNAL booster ramped multipole magnet [4].

Also, the HCX fusion experiments use pulsed quadrupoles that store about 840 times the energy of the RLA quadrupoles, but are used only for very low duty cycles (Figure 6) [5].

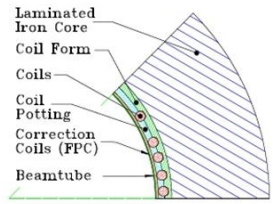

Figure 6: HCX pulsed quadrupole cross section [5].

CONCLUSION

While challenging, ramped quadrupole, dipole, and combination magnets do not appear unrealistic. Much work remains to be done to model these devices and the optics of the whole accelerator system in detail.

REFERENCES

[1] G. Wang et al., this Conference
[2] S.A. Bogacz, et al., this Conference
[3] D.J. Summers, et al., PAC 2005
[4] V.S. Kashikhin et al., PAC 2005
[5] D. Shuman, et al., PAC 2005
[7] D.J. Summers, et al., PAC 2007
[8] I.V. Bogdanov, et al., RuPAC 2008
[9] W. McLyman, Magnetic Core Selection for Transformers and Inductors, 2nd Ed., ISBN 0-8247-9841-4, p.160
[10] http://quench-analysis.web.cern.ch/quench-analysis/phd-fs-html/node7.html
[11] D.J. Summers, LEMC2007 Workshop, http://www.muonsinc.com

MULTIPASS ARC LATTICE DESIGN FOR RECIRCULATING LINAC MUON ACCELERATORS*

G.M.Wang♦, Muons, Inc., Batavia IL, and Old Dominion University, Norfolk, VA, USA
R.P. Johnson, Muons, Inc., Batavia, IL, USA
S.A Bogacz, Jefferson Lab, Newport News, VA, USA
D. Trbojevic, BNL, Upton, NY USA

Abstract

Recirculating linear accelerators (RLA) are the most likely means to achieve rapid acceleration of short-lived muons to multi-GeV energies required for Neutrino Factories and TeV energies required for Muon Colliders. A drawback of this scheme is that a separate return arc is required for each passage of the muons through the linac. In the work described here, a novel arc optics based on a Non-Scaling Fixed Field Alternating Gradient (NS-FFAG) lattice is developed, which would provide sufficient momentum acceptance to allow multiple passes (two or more consecutive energies) to be transported in one string of magnets. An RLA with significantly fewer arcs will reduce the cost. We will develop the optics and technical requirements to allow the maximum number of passes by using an adjustable path length to accurately control the returned beam to synchronize with the linac RF phase.

INTRODUCTION

In a companion paper [1], we proposed a muon RLA consisting of a single linac with pulsed quads and separate teardrop return arcs, as shown in Figure 1. That pulsed linac dogbone-shaped RLA increases the number of passes; from 8 passes to 12, leading to cost savings. However, in that scheme, one needs to separate different energy beams coming out of a linac and to direct them into appropriate droplet-shaped arcs for recirculation. Each pass through the linac would call for a separate fixed energy droplet arc, increasing the complexity of the RLA. Here, we propose to employ a novel arc optics based on a NS-FFAG [2] lattice which would provide sufficient momentum acceptance to allow multiple passes (two or more consecutive energies) to be transported in each string of magnets (single beam-line). Studies show that this arc structure is very compact and the momentum acceptance could be from -30% to +90%.

DROPLET ARC REQUIREMENTS

The new concept of a large momentum acceptance Non-Scaling FFAG-like arc in a dogbone RLA is to maximize the number of passes that $\mu^{\pm}$ can be accelerated through a single linac. The arc layout is similar to the separated arcs structure in Figure 1. It is composed of a large number of two types of unit cells, B_p and B_n, to form a closed 180 degree arc. The dipoles in unit cells B_p and B_n bend in opposite directions. The numbers of unit cells are N_p and N_n, which satisfy the requirements that the displacement in the transverse plane is $x_{dis} = 0$ and the total bending angle is $\left(N_p - N_n\right) \cdot \theta_{unit} = 180$.

In the linac, μ^+ and μ^- experience the same transport optics. After the linac, they are bent in opposite directions by the spreader bending magnet. To transport μ^+ and μ^- with the same arc structure, the arc should have these basic characteristics:

1) The arc must be achromatic and mirror symmetric, so that μ^+ and μ^- pass through the same lattice in opposite directions $\beta_s = \beta_e$, $\alpha_s = -\alpha_e$.

2) The phase advance per cell should be 90 degrees (especially in the bend plane), so that the variation of Twiss functions is minimized and it is easier to match the linac optics.

3) The beam phase relative to the SRF cavity must be accurately controlled due to the fixed RF frequency, so the path length in the arc needs to be adjustable.

Besides the above requirements for each pass, this arc also has the ability to accommodate multi-pass beam transport, i.e. large momentum acceptance. In each pass, all the above conditions should be fulfilled and the beam orbit offset should be small to make the vacuum aperture

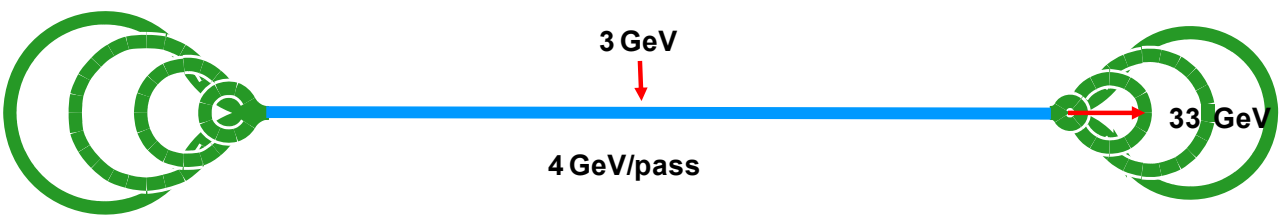

Figure 1: Layout of an 8-pass 'Dogbone' RLA with the top-to-injected energy ratio of 11.

*Supported in part by USDOE STTR Grant DE-FG02-08ER86351
♦ guimei.wang0625@gmail.com

size acceptable. The aperture for the low-momentum muon beams is determined by the muon emittances, beta functions, and dispersion.

The NS-FFAG lattice provides extremely strong focusing, resulting in very small beta functions, very small dispersion, and very small transverse aperture.

NS-FFAG BASIC CELL STUDY

The NS-FFAG basic cell [2] (assuming that the beam bends in the horizontal plane) contains a triplet magnet arrangement composed of an inward bending magnet at the center with negative gradient ("combined function" magnet, horizontally defocusing), and two outward bending magnets located at each side with positive gradient. To simplify the structure, it is symmetric with respect to the center of the middle combined function dipole (we will later see the advantage of this symmetric structure). By using a combined function magnet, the arc structure is very compact.

Assuming that the combined function magnet field is linear, we can express it as $B_y = B_0 + Gx$, $B_x = Gy$

Where, B_0 is the central field and G is the field gradient. By optimizing B_0 and magnet length, the total bend angle through one cell is

$$\theta_{unit} = \frac{L_{QD}}{\rho_{QD}} - \frac{2L_{QF}}{\rho_{QF}}$$

Once the geometric structure is set, the central field and magnet length cannot be changed, but gradients are still adjustable. By adjusting the gradients, the betatron oscillation frequencies and the dispersion can be changed.

In a periodic lattice, we can express the transverse transport matrix as

$$M = \begin{bmatrix} M_{11} & M_{12} & M_{16} \\ M_{21} & M_{22} & M_{26} \\ 0 & 0 & 1 \end{bmatrix} =$$

$$\begin{bmatrix} \cos\phi + \alpha\sin\phi & \beta\sin\phi & (1-\cos\phi-\alpha\sin\phi)D - \beta D'\sin\phi \\ -\gamma\sin\phi & \cos\phi - \alpha\sin\phi & \gamma D\sin\phi + (1-\cos\phi+\alpha\sin\phi)D' \\ 0 & 0 & 1 \end{bmatrix}$$

where β, α, γ are periodic Courant-Snyder functions, D, D' are periodic dispersion, and ϕ is the phase advance per period. The dispersion can be expressed as

$$D = \frac{M_{16}(1-\cos\phi+\alpha\sin\phi) + M_{26}\beta\sin\phi}{2(1-\cos\phi)}$$

$$D' = \frac{-M_{16}\gamma\sin\phi + M_{26}(1-\cos\phi-\alpha\sin\phi)}{2(1-\cos\phi)}$$

According to the arc requirements, we have $\phi = 90$. To simplify the dispersion match between the B_p and B_n unit cells, the achromatic lattice with $D = 0, D' = 0$ is one of the best choices. An advantage of an achromatic unit cell is that it is easy to insert dispersion-free matching cells.

A symmetric system can be treated as two mirror systems, N and N_{mirror}. The matrix M can be expressed with N as

$$M = \begin{bmatrix} 1+2N_{12}N_{21} & 2N_{12}N_{22} & 2N_{12}N_{26} \\ 2N_{11}N_{21} & 1+2N_{12}N_{21} & 2N_{11}N_{26} \\ 0 & 0 & 1 \end{bmatrix}$$

We get that $M_{11} = M_{22}$ is automatically satisfied, so $\alpha = 0$. For $D = 0, D' = 0$, we get $M_{16} = 0, M_{26} = 0$. M_{16} and M_{26} have a common item N_{26}, which lowers the number of conditions from two to one. With this symmetric structure, 90 phase advance and the achromatic condition corresponds to $N_{26} = 0$ at the middle plane and $M_{11} = 0$ for the basic cell, giving the magnet gradients as two adjustable knobs.

OPTIM has been used to optimize the lattice, where table 1 lists the magnet properties of the two basic cells designed for a 6.2 GeV muon beam. The layouts are BD-o-BF-o-BD and BDre-o-BFre-o-BDre. The drift distance o is 40cm. Comparing the focusing from bends $1/\rho^2$ and quads $G/(B\rho)$, we find that the focusing from the bends can be ignored compared to that from quads. So the quad focusing strengths are totally dominant in the optics. In the basic cells B_p and B_n, the quad strengths are the same but the bending angles are opposite.

Table 1: Combined Function Magnet Properties

Mag.	L(cm)	B(kG)	G(kG/cm)	θ(deg)
BD	0.5233	35.08	-2.28	5
BF	0.5233	-35.08	5.60	-5
BDre	0.5233	-35.08	-2.28	5
BFre	0.5233	35.08	5.60	-5

Due to the very strong focusing magnets, the beta functions and dispersion are small, as shown in Figure 2. The maximum beta functions in the x and y planes are 4.92 m and 3.39 m. The maximum and minimum dispersions are 7.21 cm and -7.21 cm. The beta functions and dispersion naturally match well for the two basic cells that bend in opposite directions.

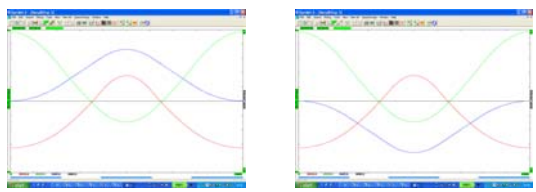

Figure 2: Beta functions and dispersion in unit cells.

To study the momentum acceptance and optics of the NS-FFAG structure for different energies, the code MADXP- Polymorphic Tracking Code (PTC) [3] is used. Since the beam energy change is large for successive passes, a perturbation method such as OPTIM for beam optics study does not work well. PTC allows symplectic

integration through all elements with user control over the precision (with full or extended Hamiltonian).

Figure 3 shows beta functions, orbit displacement, dispersion, and path length of the basic cell Bp at different energies. The energy acceptance ranges from -30% to +90% or from 4 GeV to 10.8 GeV. Based on the linac optics design in [1], this arc can accommodate at least two passes of the beam. Scaling the reference energy to 26 GeV, then the energy accommodated ranges from 18 GeV to 53 GeV. So the total number of separate arcs is reduced from 6 to 3. It can be seen that as the energy increases, the beta function changes in a small range, less than 20 m, the maximum orbit offset is about 4 cm, and the maximum dispersion is around 10 cm, which is acceptable for a large momentum muon beam. The path length changes as a parabolic function of energy rather than linearly, which allows the relative RF phase change to be limited to a small range. (Minus ds means the path length is longer than that of the reference particle.)

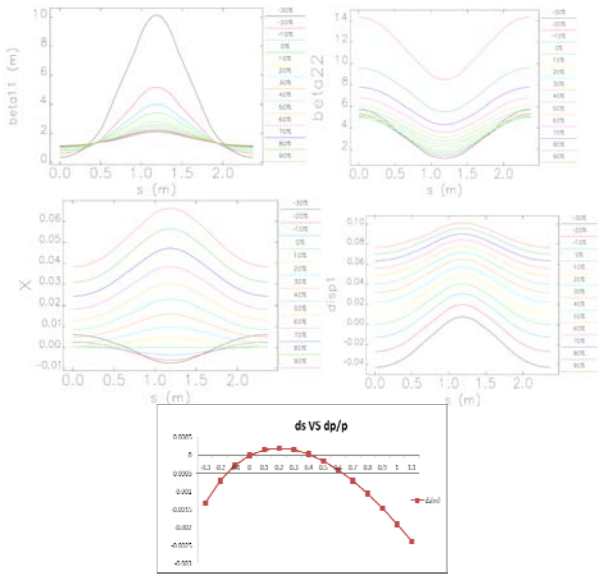

Figure 3: Beam optics for different energies at B_p cell.

For the optics of the basic cell B_n, the beta functions have the same property as those of B_p, but the orbit offset and dispersion have the opposite value, as expected since they have opposite bending. To match the dispersion, beta functions and orbit offset between unit cells B_p and B_n, the –I section should be used. Here, taking advantage of the 90 degree phase advance per cell and the very small focusing from the bend, it is easy to see that the –I section can be achieved by inserting two periods of a unit cell without bending. Here, it should be noticed that this –I section is referred to the reference particle.

Figure 4 illustrates the droplet arc optics. At the bottom the quadrupoles are depicted in red and the combined-function bending magnets in blue. Between the outward bend and inward bend section, there is a –I section. The total circumference is about 200 m with 2*60 degrees outward bend and 300 degree inward bend. This arc is very compact compared with a general FODO arc lattice, which is very important for the short lived muon beam.

To control the returned beam phase to synchronize with the RF, there are usually three ways to change path length; using an achromatic magnet structure, mechanically moving the arc, or changing the RF wavelength. Considering this RLA structure is to accelerate muon beams in two directions in a large arc, the best choice to adjust path length is using an achromatic structure. A chicane structure [4] is very simple, with the property that the higher energy, the shorter the path length. It is widely used in various facilities. Figure 3 shows that the path length change as a function of energy is a parabolic curve. For one arc to transport two passes, it is best that the energy of the two passes is located at two sides of the curve, symmetric about the peak, so that the path length change due to the chicane can be minimized.

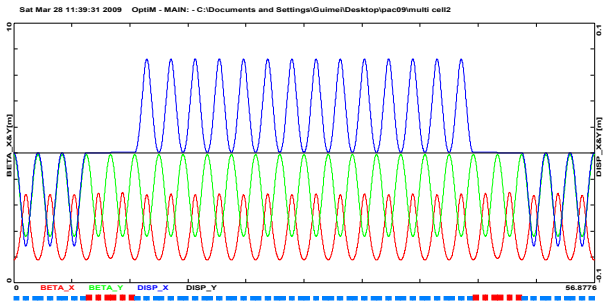

Figure 4: Droplet arc optics.

CONCLUSION

A droplet arc based on a NS-FFAG lattice has been designed to transport multipass beams, lowering the number and hence the total cost of the arcs for a muon RLA. Studies show that such a lattice can accommodate beam energies over a very large range and have the property of small beta functions and small dispersion due to the strong focusing of a NS-FFAG. The special optics match required inside the droplet structure is solved by inserting –I section. To synchronize the beam phase with RF, a chicane structure is adopted to adjust beam path length.

More studies will be investigated to scale this design to higher energy and to improve the matching of the beam optics between the arc and linac.

REFERENCES

[1] S.A. Bogacz et al., this conference
[2] D. Trbojevic, E. Courant, and M. Blaskiewicz, Phys. Rev. ST Accelerators and Beams 8, 050101 (2005).
[3] Maxdp, http://mad.web.cern.ch/mad/
[4] Guimei Wang, Ph.D. thesis, 2008
[5] Alexander W. Chao and Maury Tigner, Handbook of Acc. Physics and Engineering, World Scientific, 1999

PULSED-FOCUSING RECIRCULATING LINACS FOR MUON ACCELERATION*

S.A. Bogacz♦, Jefferson Lab, Newport News, VA, USA
G. Wang, Muons, Inc., Batavia IL, and Old Dominion University, Norfolk, VA, USA
R.P. Johnson, Muons, Inc., Batavia IL, USA.

Abstract

Neutrino Factories and Muon Colliders require rapid acceleration of short-lived muons to multi-GeV and TeV energies. A Recirculating Linear Accelerator (RLA) that uses superconducting RF structures can provide exceptionally fast and economical acceleration to the extent that the focusing range of the RLA quadrupoles allows each muon to pass several times through each high-gradient cavity. A new concept of rapidly changing the strength of the RLA focusing quadrupoles as the muons gain energy is being developed to increase the number of passes that each muon will make in the RF cavities, leading to greater cost effectiveness. We discuss the optics and technical requirements for RLA designs, using RF cavities capable of simultaneous acceleration of both μ^+ and μ^- species, with pulsed Linac quadrupoles to allow the maximum number of passes. The design will include the optics for the multi-pass linac and droplet-shaped return arcs [1].

MULTI-PASS LINAC OPTICS

The superconducting accelerating structure is by far the most expensive component of the accelerator complex. Maximizing the number of passes in the RLA can significant lower the cost [2] of the overall acceleration scheme.

The RLA linac consists of uniformly spaced RF cavities phased for a speed-of-light particle. The injection energy into the RLA and the energy gain per linac pass were optimized so that a tolerable level of RF phase slippage along the linac could be maintained. Furthermore, to minimize phase slippage at the lowest energy pass, an injection at the middle of the linac was chosen.

The key element of the transverse beam dynamics in a multi-pass 'Dogbone' RLA is an appropriate choice of multi-pass linac optics. The focusing profile along the linac (quadrupole gradients) needs to be set, so that one can transport (i.e. provide adequate transverse focusing for a given aperture) multiple pass beams within a very large energy range.

Since the beam is traversing the linac in both directions throughout the course of acceleration, one would like to maintain a 90° phase advance per cell for the lowest energy pass (the initial half-pass) by scaling the quad gradients with increasing energy along the linac. In order to mitigate the beta beating due to reduced focusing for the subsequent passes, the other half of the linac would have the inverted scaling of the quadrupole gradients. The resulting mirror symmetric focusing profile of the linac is illustrated in Figure 2.

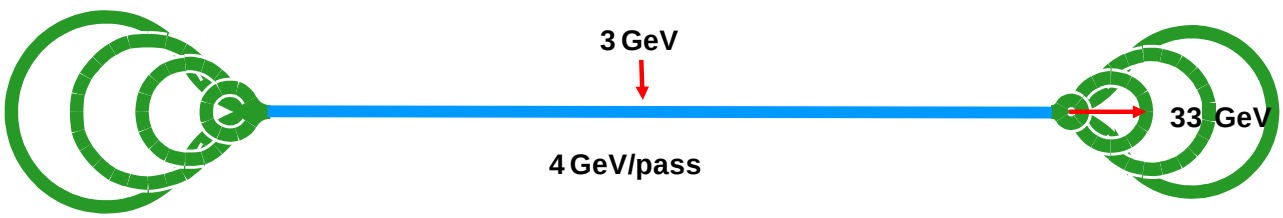

Figure 1: The RLA layout features a 'Dogbone' based on a 250 meter long linac (20 FODO; 4 RF cavities/cell).

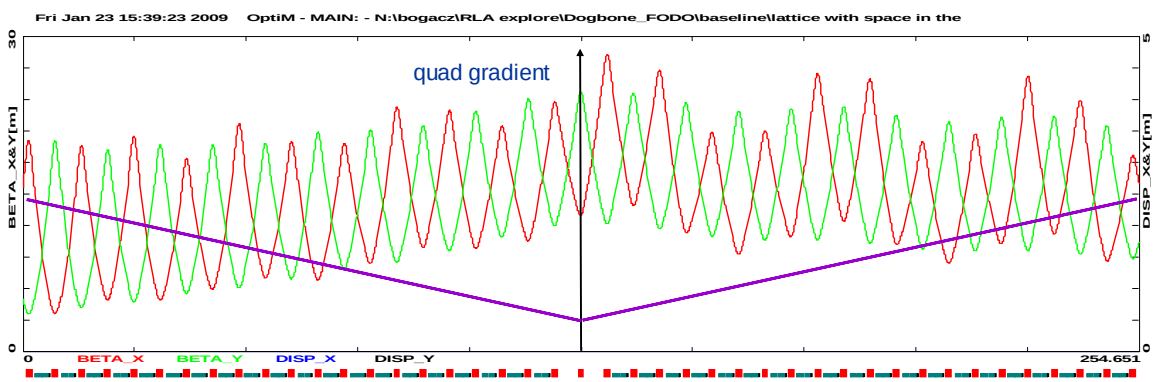

Figure 2: Bisected linac Optics – mirror symmetric quadrupole gradient profile minimizing under-focus beta beating.

*Supported in part by US DOE-STTR Grant DE-FG02-08ER86351
and JSA DOE Contract No. DE-AC05-06OR23177
♦bogacz@jlab.org

Now we consider a 'Pulsed' linac Optics for the same RLA layout. Here we assume a time varying quad strength in the RLA linac described in the previous section. A feasible quad pulse would assume a 500 Hz cycle ramp with the top pole field of 1 Tesla. That would translate to a maximum quad gradient of G^{max} =2 kGauss/cm (5 cm bore radius) ramped over τ = 1 ms from the initial gradient of G_0 =0.1 kGauss/cm. We have used a fairly conservative rise time based on similar applications for ramping the new corrector magnets for the Fermilab Booster that have 1 kHz capability [3].

For simplicity, we consider a linear ramp according to the following formula:

$$G(t) = G_0 + \frac{G^{max} - G_0}{\tau} t \qquad (1)$$

A single bunch travelling with a speed of light along the linac with quads ramped according to Eq.(1), 'sees' the following quad gradient passing through the i-th cell along the linac (i = 1,…20)

$$G_i = G_0 + \frac{G^{max} - G_0}{\tau} \frac{\ell_{cell}}{c} i \qquad (2)$$

where ℓ_{cell} is the cell length and i defines the bunch position along the linac.

For multiple passes through the linac (the index n defines the pass number) the above formula can be generalized as follows:

$$G_i^n = G_0 + \frac{G^{max} - G_0}{\tau c}\left[(n-1)\left(\ell_{linac} + \frac{n}{2}\ell_{arc}\right) + i\ell_{cell}\right] \qquad (3)$$

where ℓ_{linac} is the full linac length and ℓ_{arc} is the length of the lowest energy droplet arc. Here we also assume that the energy gain per linac is much larger than the injection energy. Figure 3 illustrates the multi pass optics for the pulsed linacs. As one can see below, there is sufficient phase advance to support up to 12 passes.

Pass 8 (31-35 GeV)

Fixed

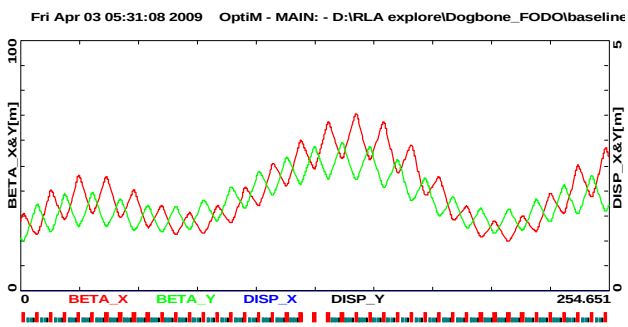

Pulsed

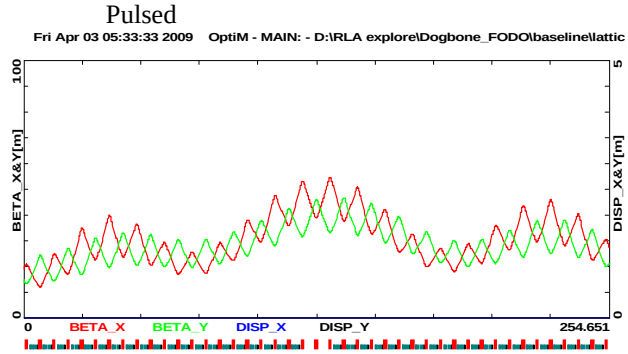

Pass 12 (47-51 GeV)

Fixed

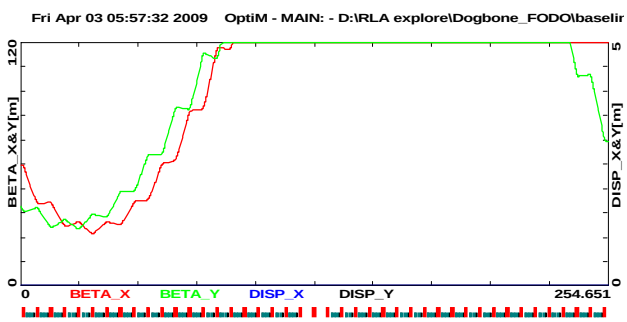

Pulsed

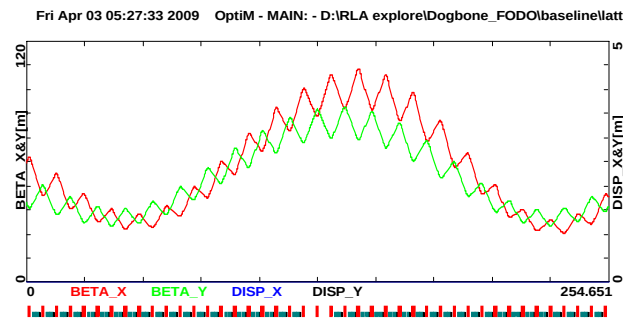

Figure 3: The 8-th pass and the last one (12-th) of the pulsed linac optics. By pulsing the focusing quads as described in Eq.(3), the additional 4 passes increase the output energy from 35 to 51 GeV. Red is horizontal and green is vertical.

'DROPLET' ARCS

In a 'Dogbone' RLA one needs to separate different energy beams coming out of a linac and to direct them into appropriate 'droplet' arcs for recirculation [1]. For multiple practical reasons, horizontal rather than vertical beam separation was chosen. Rather than suppressing horizontal dispersion created by the Spreader, it is smoothly matched to the horizontal dispersion of the outward 60^0 arc. Then by the appropriate pattern of removed dipoles in three transition cells, one 'flips' the dispersion for the inward bending 300^0 arc, etc. The entire 'droplet' Arc optics architecture is based on 90^0 betatron phase advance cells with uniform periodicity of Twiss functions. The resulting 'droplet' Arc optics based on FODO focusing [2] is illustrated along with its 'footprint' in Figure 4.

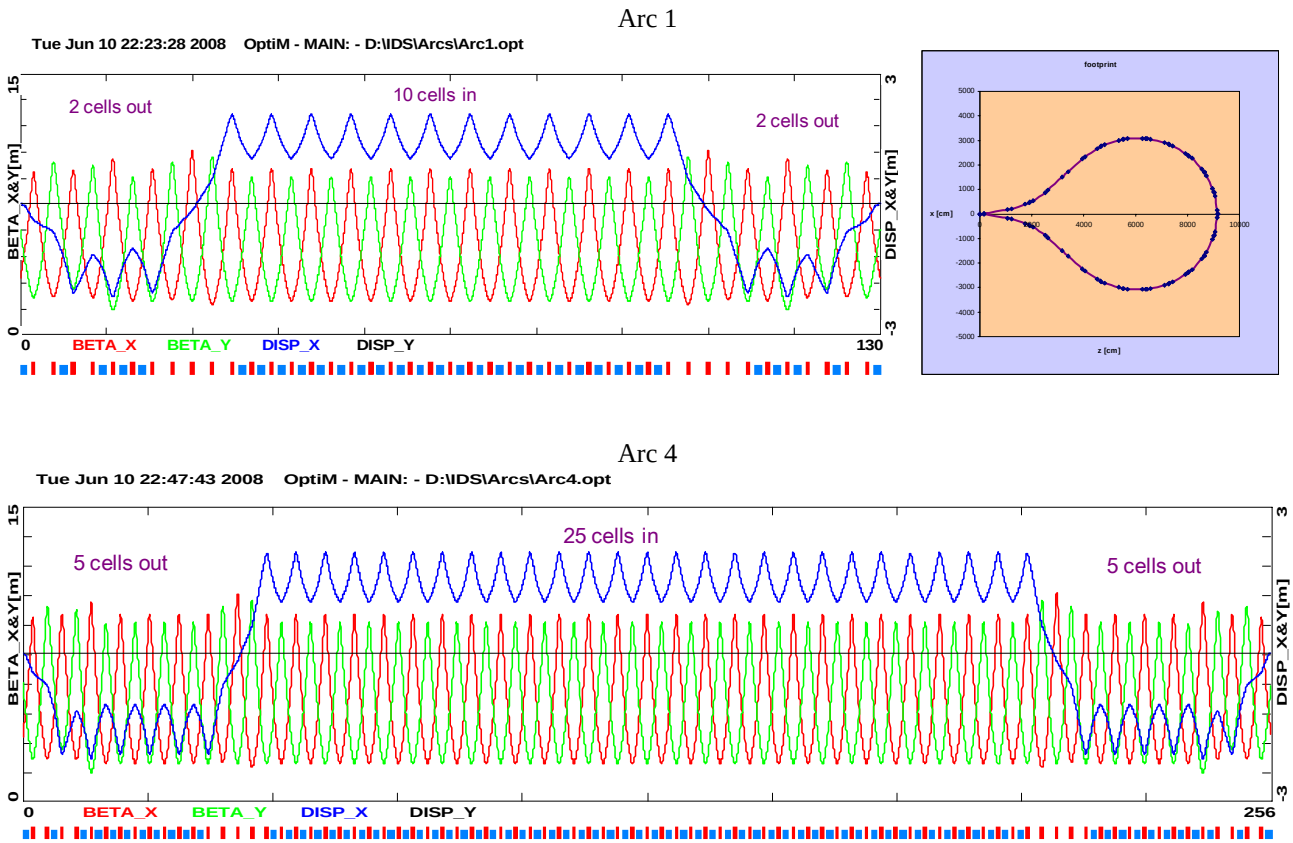

Figure 4: 'Droplet' Arc optics and its 'footprint' – uniform periodicity of beta functions and dispersion. The design offers both compactness and modularity; the top plot illustrates the lowest energy arc.The higher arcs based on the same bending field are configured by adding periodic cells in the outward and inward bending sections, extending the circumference and increasing the quadrupole strength according to the momentum. The bottom plot illustrates Arc 4 Optics.

CONCLUSIONS

A Recirculating Linear Accelerator (RLA) can provide exceptionally fast and economical acceleration to the extent that the focusing range of the RLA quadrupoles allows each muon to pass several times through each high-gradient cavity. A new concept of rapidly changing the strength of the RLA focusing quadrupoles as the muons gain energy has been developed. It significantly increases the number of passes that each muon will make in the RF cavities, leading to greater cost effectiveness. A complete linear lattice for the RLA has been designed (multi pass-linac with pulsed quads and 12 droplet arcs) Technical feasibility, ultimate limitations, and cost effectiveness of such schemes is presently under studies [4], [5].

REFERENCES

[1] S.A. Bogacz, Nuclear Physics B, Vol **155**, 334, (2006)
[2] J.S. Berg et al., Physical Review Special Topics – Accelerators and Beams, **9**, 011001 (2006)
[3] V.S. Kashikhin et al., PAC 2005
[4] G. Wang et al., this Conference
[5] K. Beard et al., this Conference

MUON ACCELERATION WITH RLA AND NON-SCALING FFAG ARCS*

V.S. Morozov#, Old Dominion University, Norfolk, VA, USA & Muons, Inc.
S.A. Bogacz, Jefferson Lab, Newport News, VA, USA
Dejan Trbojevic, BNL, Upton, NY USA

Abstract

Recirculating Linear Accelerators (RLA) are the most likely means to achieve the rapid acceleration of short-lived muons to multi-GeV energies required for Neutrino Factories and TeV energies required for Muon Colliders. In this paper, we present a novel return-arc optics design based on a Non Scaling Fixed Field Alternating Gradient (NS-FFAG) lattice that allows 5 and 9 GeV/c muons of both charges to be transported in the same string of magnets. The return arcs are made up of super cells with each super cell consisting of three triplets. By employing combined function magnets with dipole, quadrupole, sextupole and octupole magnetic field components, each super cell is designed to be achromatic and to have zero initial and final periodic orbit offsets for both 5 and 9 GeV/c muon momenta. This solution would reduce the number of arcs by a factor of 2, simplifying the overall design.

INTRODUCTION

Figure 1 shows a proposed [1] dog-bone-shaped muon RLA consisting of a single linac with pulsed quads and separate droplet return arcs. In the example illustrated in Fig. 1, the number of passes is increased by pulsing linac quads from 8 passes to 12, leading to significant cost savings. However, in that scheme, one needs to separate different energy beams coming out of the linac and to direct them into appropriate droplet-shaped arcs for recirculation. Each pass through the linac would call for a separate fixed energy droplet arc, increasing the complexity of the RLA. Here, we propose a novel return-arc optics design based on a Non-Scaling Fixed Field Alternating Gradient [2] (NS-FFAG) lattice, which allows two (potentially even more) consecutive passes with very different energies to be transported through the same string of magnets.

DROPLET ARC REQUIREMENTS

Through use of large momentum acceptance NS-FFAG arcs in a dogbone RLA, one can maximize the number of passes that $\mu^{\pm}$ can be accelerated through a single linac. The arc layout is similar to the separated arcs structure in Fig. 1. Each droplet arc consists of a 60° outward bend, a 300° inward bend and another 60° outward bend so that the net bend is 180°. This arc geometry has the advantage that if the outward and inward bends are made up of similar cells, the geometry automatically closes without the need for any additional straight sections, thus making it simpler and more compact.

To transport different energy muons of both charges through the same arc structure, the arc must possess the following properties:

1) For each transported momentum, the periodic orbit's offset must be zero at the arc's entrance and exit to ensure that the beam goes through the center of the linac.
2) The arc must be achromatic for each momentum to guarantee matching to the linac.
3) The arc must be mirror symmetric, so that μ^+ and μ^- can pass through the same lattice in opposite directions. The symmetry ensures that the periodic beta functions are identical at the arc's ends and that the periodic alpha functions and dispersion slope are zero at the ends.
4) The arc must be near isochronous for both energies to ensure proper phasing with the linac.
5) The orbit offsets as well as beta functions and dispersion for both energies should be small enough to keep the aperture size acceptable.

This proposed NS-FFAG lattice meets all these requirements.

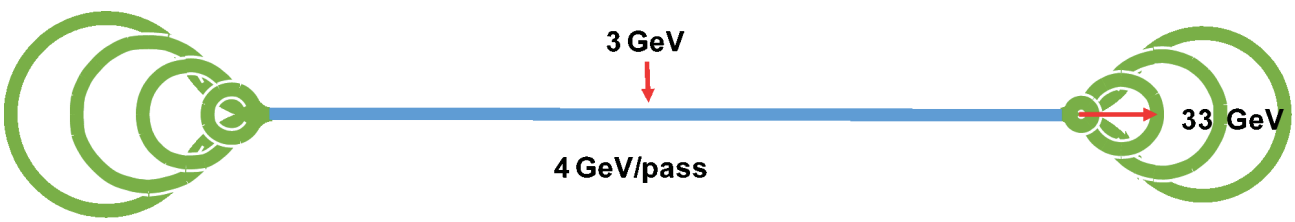

Figure 1: Layout of an 8-pass 'Dogbone' RLA with the top-to-injected energy ratio of 11.

* Supported in part by US DOE STTR Grant DE-FG02-08ER86351
# morozov@jlab.org

ARC DESIGN BASED ON NS-FFAG CELL

As a basis of our droplet arc design, we used the NS-FFAG [2] triplet magnet arrangement, which was extensively studied in [3]. The outward-bending triplet cell consists of an inward bending combined function magnet with positive gradient (horizontally focusing) at the center and two outward bending magnets located on either side with equal negative gradients. The inward-bending triplet cell has the same structure but reversed dipole fields. The fact that the cells are symmetric with respect to their centers ensures that their periodic solutions have $\alpha_x = \alpha_y = 0$ and $D'_x = 0$ at the beginning and the end of the cells. It was demonstrated in [3] that, by using combined function magnets, the arc structure can be made very compact and that such a lattice can accommodate beam energies over a very large range and is characterized by small beta functions and small dispersion due to the strong focusing of a NS-FFAG.

The study reported in [3] considered combined function magnets with dipole and quadrupole magnetic field components only. It was found that, despite a large momentum acceptance, the off-momentum periodic orbit's offset and the off-momentum periodic dispersion were not zero at the entrance and exit of the triplet cells making matching the cells to the linac and matching the outward bending cells to the inward bending cells difficult. Thus, in our study we used combined function magnets, which in addition to the dipole and quadrupole components, also included sextupole and octupole ones.

To study the optics of the NS-FFAG structure for large momentum range, we used the Polymorphic Tracking Code (PTC) module of the MAD-X program [4]. While perturbative method codes are not suitable for such a study, PTC allows symplectic integration through all elements with user control over the precision (with full or expanded Hamiltonian).

For simplicity we made 5 GeV/c the nominal momentum going through the magnet centers. The constraint that the 5 GeV/c periodic orbit has to have zero offset coming in and out of the cell is then automatically satisfied. Besides, once the 5 GeV/c linear optics is adjusted with quadrupole gradients, introduction of the sextupole and octupole magnetic field components required for accommodating the 9 GeV/c momentum does not change it. This decouples the 5 GeV/c linear optics from the 9 GeV/c optics and ensures that, once the $D_x = 0$ and $D'_x = 0$ conditions are satisfied with the quadrupole gradients at 5 GeV/c, they are not affected by tuning of the 9 GeV/c linear optics with the sextupole and octupole components.

For the triplets, we chose 1 m long magnets separated by 20 cm gaps. To simplify the geometry, each magnet's bending angle was set to 5°. We then adjusted the quadrupole gradients to make the triplet cell achromatic. The quadrupole gradient of the middle magnet was adjusted as strong as possible without losing transverse motion stability in order to minimize the 9 GeV/c orbit offset. This determined the cell's phase advance. Figures 2 and 3 show the 9 GeV/c period orbit, beta functions, and dispersion for the outward and inward bending cells, respectively. Note that, since there is no coupling in our case, the Ripken's β_{11} and β_{22} are simply equal respectively to the usual horizontal and vertical beta-functions. Comparing Figs. 2 and 3, one can see that the beta functions for the two cell types are the same while the dispersion changes sign. Since the cells are achromatic, they can be matched together in a natural way.

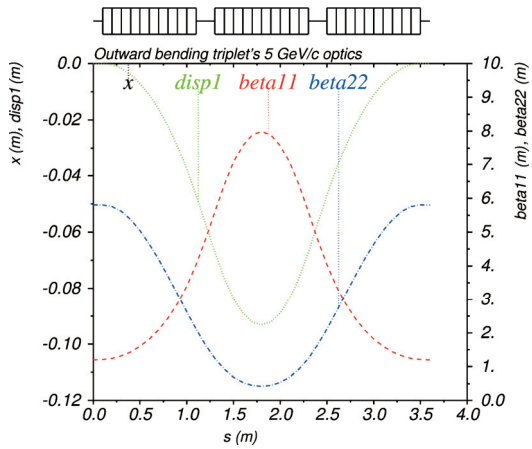

Figure 2: 5 GeV/c periodic orbit, dispersion and beta functions of the outward bending triplet cell.

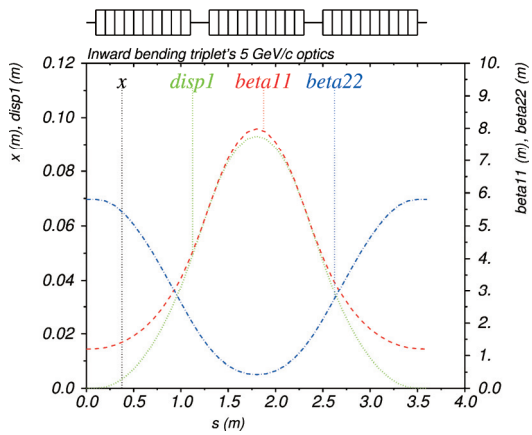

Figure 3: 5 GeV/c periodic orbit, dispersion and beta functions of the inward bending triplet cell.

We next studied the triplet cell's 9 GeV/c optics by introducing sextupole components in the cell's magnets in a symmetric way. The 9 GeV/c periodic orbit's deviation is large in the middle magnet and is much smaller in the side magnets. Therefore, the effect of the sextupole component is large in the middle magnet and is almost negligible in the side magnets. For this reason, it was not possible to satisfy, at the same time, the zero orbit offset and achromatic conditions by adjusting the sextupole components of the middle and side magnets.

Therefore, we combined three triplet cells into a super cell. The sextupole strength of the middle magnets of the two outer triplet cells was used as one parameter. The sextupole strength of the middle magnet of the central triplet cell was the second parameter. This arrangement preserves the super cell's mirror symmetry. By varying the above two parameters, we were able to simultaneously satisfy the conditions of the super cell being achromatic and having zero incoming and outgoing periodic orbit offset. To keep the transverse motion stable in both

dimensions, we added small octupole components of the same strength to the center magnets of all three triplets. This modified the field gradient along the 9 GeV/c reference orbit in these magnets restoring the stability. The periodic orbit and dispersion of the outward bending super cell are shown in Fig. 4. Figure 5 illustrates the 9 GeV/c beta functions of that type of cell. Figures 6 and 7 show similar graphs for the inward bending super cell. Figures 4-7 demonstrate that changing the bending direction does not affect the beta functions, but reverses the signs of the periodic orbit and dispersion. Since the super cell is achromatic and has zero incoming and outgoing periodic orbit offset, it is clear that the super cells are automatically matched. Since the net bend of each super cell is 15°, they can be easily put together to form the 60° and 300° bends of the droplet arc.

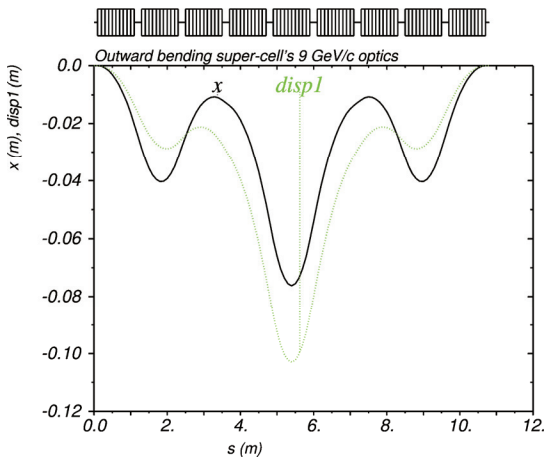

Figure 4: 9 GeV/c periodic orbit and dispersion of the outward bending super cell.

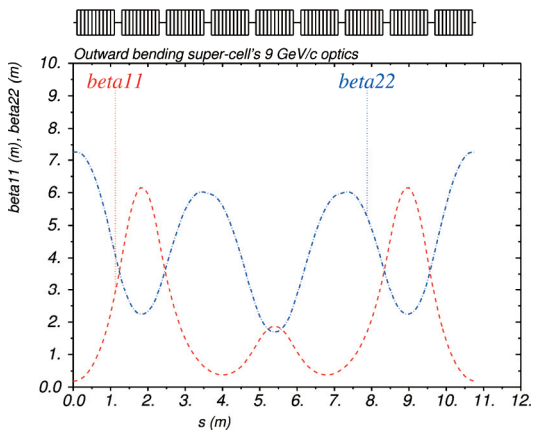

Figure 5: 9 GeV/c beta functions of the outward bending super cell.

This design can be further optimized to minimize the orbit offset and the required magnetic fields. One can consider including more triplets in the super cell. Another path for improvement is to choose the reference momentum to be between 5 and 9 GeV/c. This would also allow one to adjust the path lengths to make the arc closer to isochronous for the different momenta. The non-linear effects and the dynamic aperture are being studied.

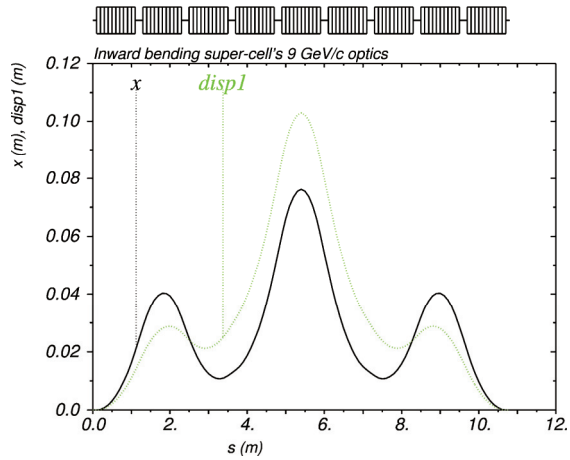

Figure 6: 9 GeV/c periodic orbit and dispersion of the inward bending super cell.

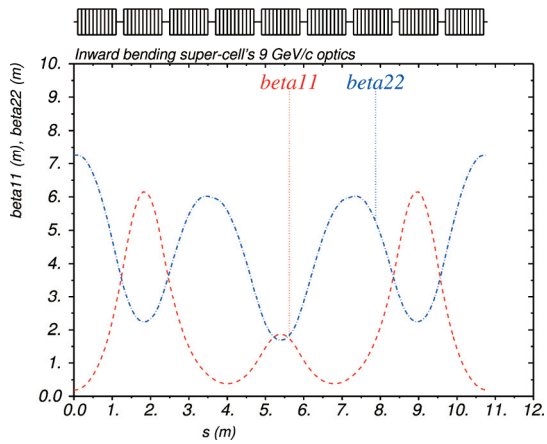

Figure 7: 9 GeV/c beta functions of the inward bending super cell.

CONCLUSION

A droplet arc design based on a NS-FFAG lattice has been developed to transport both 5 and 9 GeV/c muon beams of both charges. This lowers the number of arcs and eases the design of a muon RLA. The arc properties of being achromatic and having zero periodic orbit offset for the two momenta facilitates matching of the arc to the linac. As the next step, we plan to study matching of our NS-FFAG arc to the multi-pass linac optics by lifting the symmetry requirements in some of the cells adjacent to the droplet arc ends and using the additional parameters to satisfy the matching conditions.

REFERENCES

[1] S.A. Bogacz et al., "Pulsed-focusing recirculating linacs for muon acceleration", in Proc. PAC 09, Vancouver, BC, Canada.
[2] D. Trbojevic, E. Courant, and M. Blaskiewicz, Phys. Rev. ST Accel. Beams 8, 050101 (2005).
[3] G.M. Wang et al., "Multipass arc lattice design for recirculating linac muon accelerators", in Proc. PAC 09, Vancouver, BC, Canada.
[4] MAD-X, http://mad.web.cern.ch/mad/.

RECIRCULATING LINEAR ACCELERATORS FOR FUTURE MUON FACILITIES*

S.A. Bogacz♦, Jefferson Lab, Newport News, VA, USA
K.B.Beard, R.P. Johnson, Muons, Inc., Batavia, IL, USA

Abstract

Neutrino Factories (NF) and Muon Colliders (MC) require rapid acceleration of short-lived muons to multi-GeV and TeV energies. A Recirculating Linear Accelerator (RLA) that uses superconducting RF structures can provide exceptionally fast and economical acceleration to the extent that the focusing range of the RLA quadrupoles allows each muon to pass several times through each high-gradient cavity. A new concept of rapidly changing the strength of the RLA focusing quadrupoles as the muons gain energy is being developed to increase the number of passes that each muon will make in the RF cavities, leading to greater cost effectiveness.

ACCELERATION SCHEME OVERVIEW

To provide sufficient muon flux for either a MC or NF will require a high power proton driver over 4 MW of beam power at some energy greater than 6 GeV.

Intense proton bunches are tightly focused onto a target capable of many MW operation to produce an intense pion beam. The pions are captured in a strong solenoidal field where they decay into muons (and neutrinos). At the end a 40 m pion decay channel the muon beam has transverse normalized emittances of around 40,000 mm-mr and is spread in time over tens of ns. The transverse dimensions of the beam must be cooled to be small enough and bunches must formed to fit into reasonable accelerating structures. For a MC, this is about a factor of a thousand in each transverse plane, or a factor of a million in six-dimensional emittance reduction.

3 GEV LINEAR PRE-ACCELERTOR

A single-pass linac "pre-accelerator" raises the beam energy to 3 GeV. This makes the muons sufficiently relativistic to facilitate further acceleration in a RLA. In addition, the longitudinal phase space volume is adiabatically compressed in the course of acceleration [1]. The large acceptance of the pre-accelerator requires large aperture and tight focusing at its front-end. Given the large aperture, tight space constraints, moderate beam energies, and the necessity of strong focusing in both planes, we have chosen solenoidal focusing for the entire linac [3]. The beam size is adiabatically damped with acceleration, and that allows the short cryo-modules to be replaced with the intermediate

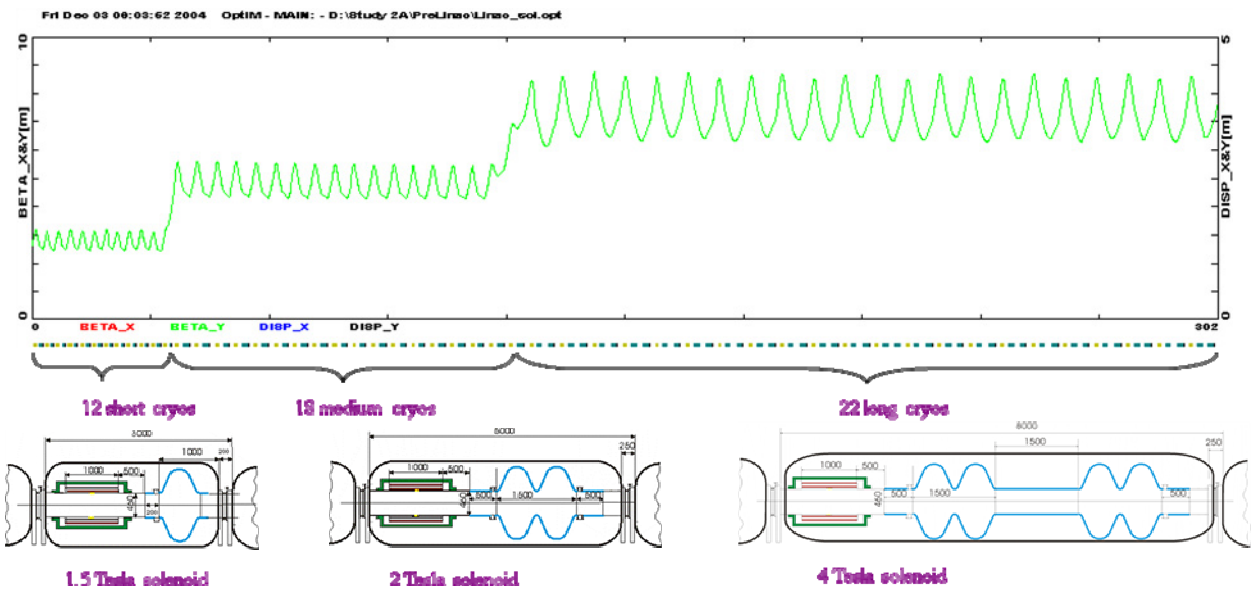

Figure 1: Transverse optics– uniform periodic focusing with 12 short, 18 medium, and 22 long cryo-modules.

and finally long cryo-modules as illustrated in Fig. 1. In the initial part of the linac, when the beam is still not completely relativistic, the offcrest causes synchrotron motion which allows bunch compression in both length and momentum spread. The synchrotron motion also suppresses the sag in acceleration for the bunch head and tail.

*Supported in part by US DOE-STTR Grant DE-FG02-08ER86351 and JSA DOE Contract No. DE-AC05-06OR23177
♦bogacz@jlab.org

There is a 0.4% beam loss coming mainly from particles at the longitudinal phase space boundary.

MULTI-PASS LINAC OPTICS

The superconducting accelerating structure is by far the most expensive component of the accelerator complex. Maximizing the number of passes in the RLA can significant lower the cost [2] of the overall acceleration scheme.

There are two notable advantages of the 'Dogbone' configuration compared to the 'Racetrack': better orbit separation at the linac ends resulting from larger (factor of two) energy difference between two consecutive linac passes. Furthermore, more favorable optics solution for simultaneous acceleration of both $\mu^{\pm}$ species can be supported by the 'Dogbone topology', which allows both charge species to traverse the RLA linac in the same direction.

The key element of the transverse beam dynamics in a multi-pass 'Dogbone' RLA is an appropriate choice of multi-pass linac optics. Since the beam is traversing the linac in both directions throughout the course of acceleration, one would like to maintain a 90° phase advance per cell for the lowest energy pass (the initial half-pass) by scaling the quad gradients with increasing energy along the linac. In order to mitigate the beta beating due to reduced focusing for the subsequent passes, the other half of the linac would have the inverted scaling of the quadrupole gradients, as illustrated in Figure 3.

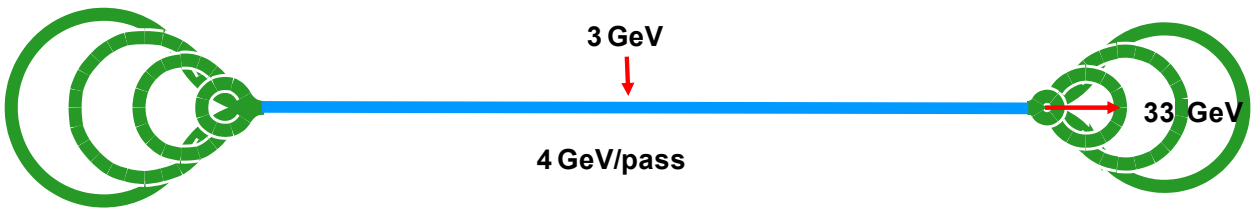

Figure 2: The RLA layout features a 'Dogbone' based on a 250 meter long linac (20 FODO; 4 RF cavities/cell).

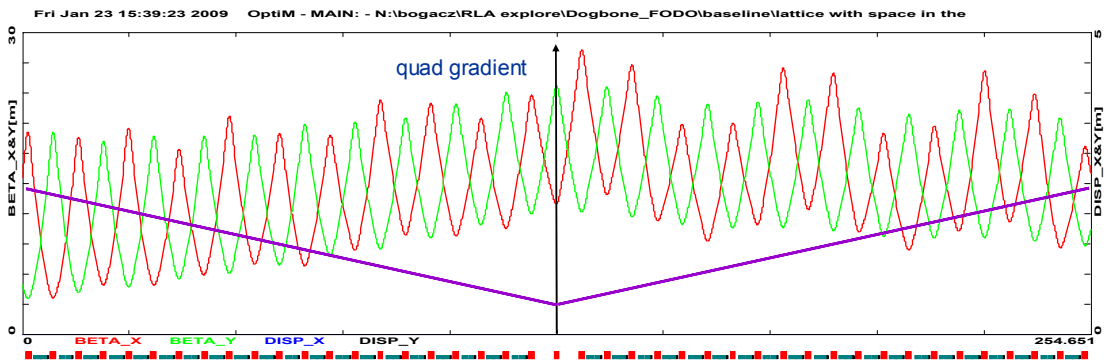

Figure 3: Bisected linac Optics – mirror symmetric quadrupole gradient profile minimizing under-focus beta beating.

Now we consider a 'Pulsed' linac Optics for the same RLA layout. Here we assume a time varying quad strength in the RLA linac described in the previous section. A feasible quad pulse would assume a 500 Hz cycle ramp with the top pole field of 1 Tesla. That would translate to a maximum quad gradient of G^{max} =2 kGauss/cm (5 cm bore radius) ramped over τ = 1 ms from the initial gradient of G_0 =0.1 kGauss/cm.

Figure 4 illustrates the multi pass optics for the pulsed linacs. As one can see below, there is sufficient phase advance to support up to 12 passes.

Pass 8 (31-35 GeV): Fixed Pulsed

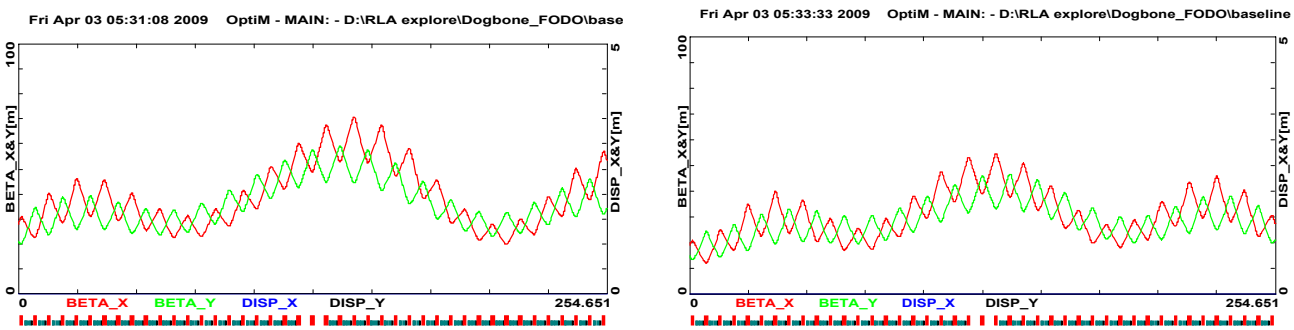

Pass 12 (47-51 GeV): Fixed Pulsed

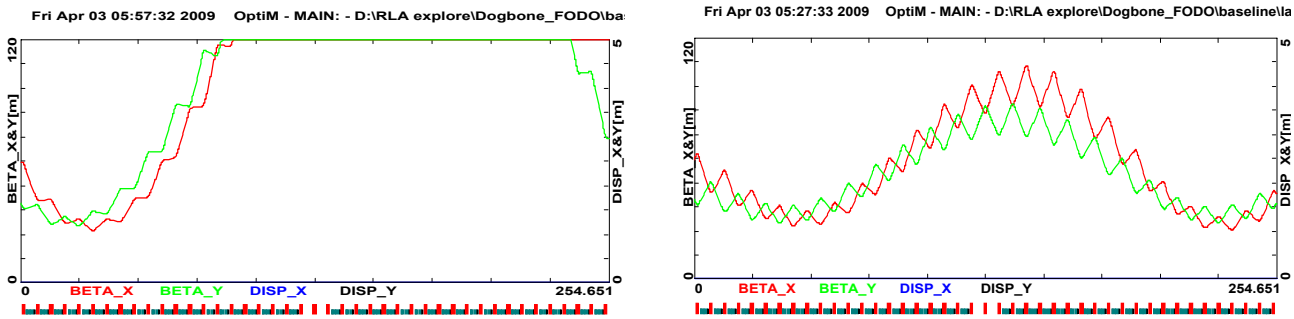

Figure 4: The 8-th pass and the last one (12-th) of the 'fixed' vs 'pulsed' linac optics - additional 4 passes gained.

'DROPLET' ARCS

In a 'Dogbone' RLA one needs to separate different energy beams coming out of a linac and to direct them into appropriate 'droplet' arcs for recirculation [1]. Rather than suppressing horizontal dispersion created by the Spreader, it is smoothly matched to the horizontal dispersion of the outward 60^0 arc. Then by the appropriate pattern of removed dipoles in three transition cells, one 'flips' the dispersion for the inward bending 300^0 arc, etc. The entire 'droplet' Arc optics architecture is based on 90^0 betatron phase advance cells with uniform periodicity of Twiss functions. The resulting 'droplet' Arc optics based on FODO focusing [2] is illustrated along with its 'footprint' in Figure 5.

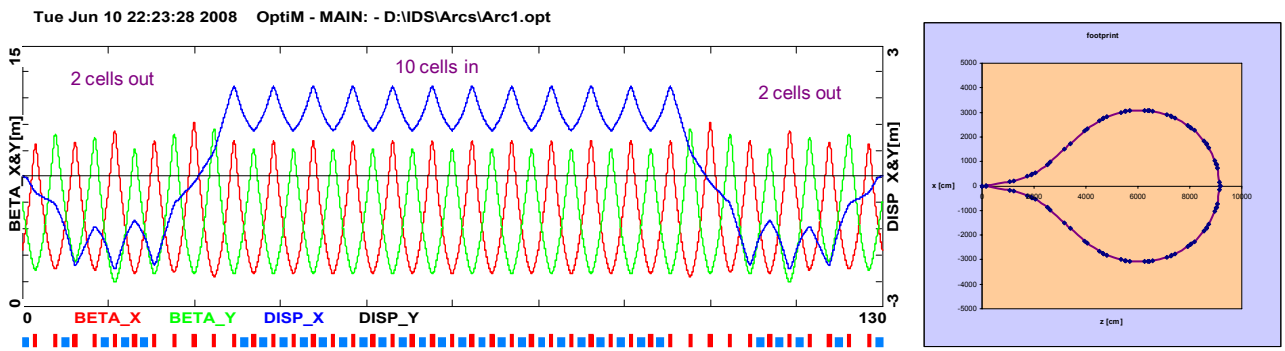

Figure 5: 'Droplet' Arc optics and its 'footprint' – uniform periodicity of beta functions and dispersion.

MULTI-PASS FFAG ARCS

Usage of pulsed quad focusing in the linac increased number of passes significantly, leading to cost savings. However, one needs to separate different energy beams coming out of a linac and to direct them into appropriate droplet-shaped arcs for recirculation. Each pass through the linac would call for a separate fixed energy droplet arc, increasing the complexity of the RLA. We also consider a novel return-arc optics design [4,5] based on a Non-Scaling Fixed Field Alternating Gradient (NS-FFAG) lattice, which allows two (potentially even more) consecutive passes with very different energies to be transported through the same string of magnets.

CONCLUSIONS

Recirculating Linear Accelerators (RLAs) can provide exceptionally fast and economical muon acceleration. They are limited to the extent that the focusing range of the RLA quadrupoles allows each muon to pass several times through each high-gradient cavity and by the return arcs. The new concepts of rapidly changing the strength of the RLA focusing quadrupoles and use beta function beating as the muons gain energy has been developed that significantly increases the number of passes that each muon will make in the RF cavities

A droplet arc design based on a NS-FFAG lattice has been developed to transport muon beams of two passes for both charge species. This lowers the number of arcs and eases the design of a muon RLA. A droplet arc based on NS-FFAG lattice, allowing two consecutive passes with different energies to be transported through the same beamline is being considered.

REFERENCES

[1] S.A. Bogacz, Nuclear Physics B, Vol 155, 334, (2006).
[2] J.S. Berg et al., Physical Review Special Topics – Accelerators and Beams, 9, 011001 (2006).
[3] S.A. Bogacz et al, PAC09.
[4] G. Wang et al, PAC09.
[5] V. Morozov et al., this Conference.

MULTIPASS MUON RLA RETURN ARCS BASED ON LINEAR COMBINED-FUNCTION MAGNETS*

V.S. Morozov#, S.A. Bogacz, Y.R. Roblin, Jefferson Lab, Newport News, VA, USA
K.B. Beard, Muons, Inc., Batavia, IL, USA

Abstract

Recirculating Linear Accelerators (RLA) are an efficient way of accelerating short-lived muons to the multi-GeV energies required for Neutrino Factories and TeV energies required for Muon Colliders. In this paper we present a design of a two-pass RLA return arc based on linear combined function magnets, in which both charge muons with momenta different by a factor of two are transported through the same string of magnets. The arc is composed of 60°-bending symmetric super cells allowing for a simple arc geometry closing. By adjusting the dipole and quadrupole components of the combined-function magnets, each super cell is designed to be achromatic and to have zero initial and final periodic orbit offsets for both muon momenta. Such a design provides a greater compactness than, for instance, an FFAG lattice with its regular alternating bends and is expected to possess a large dynamic aperture characteristic of linear-field lattices.

INTRODUCTION

Figure 1 shows a schematic layout of a dog-bone-shaped muon RLA [1] consisting of a single linac with droplet return arcs. Reusing the same linac for multiple beam passes provides for a more compact accelerator design and leads to significant cost savings. In the conventional scheme with separate return arcs, different energy beams coming out of the linac are separated and directed into appropriate arcs for recirculation. Each pass through the linac requires a separate fixed-energy arc, increasing the complexity of the RLA. We present a novel return-arc optics design based on linear combined functions magnets with variable dipole and quadrupole field components, which allows two consecutive passes with very different energies to be transported through the same string of magnets.

In the scheme illustrated in Fig. 1, a 0.9 GeV/c muon beam is injected in the middle of a 0.6 GeV/pass linac. The linac is then traversed by the beam four times. Therefore, one of the return arcs accommodates 1.2 and 2.4 GeV/c muon momenta, while the other arc accommodates 1.8 and 3.0 GeV/c momenta. The two arcs can be designed using the same approach. Below we will focus our discussion on the 1.2/2.4 GeV/c arc whose design is somewhat more challenging due to the greater fractional momentum difference of the two passes.

OPTICS DESIGN

Arc Design Concept

Each droplet arc consists of a 60° outward bend, a 300° inward bend and another 60° outward bend so that the net bend is 180°. This arc geometry has the advantage that if the outward and inward bends are composed of similar cells, the geometry automatically closes without the need for any additional straight sections, making it simpler and more compact.

The super cells constituting the arc are designed to satisfy the following basic conditions:

- Each super cell possesses periodic solutions for the orbit and the Twiss functions.
- At the beginning and at the end of each super cell, the periodic orbit offset, dispersion and their slopes are all zero.

These conditions are met at both momenta. The former condition ensures that the super cells bending in the same direction are optically matched while the latter one ensures optical matching of the cells bending in the opposite directions. The latter condition also implies that the beam is centered in the linac and that the linac is dispersion free.

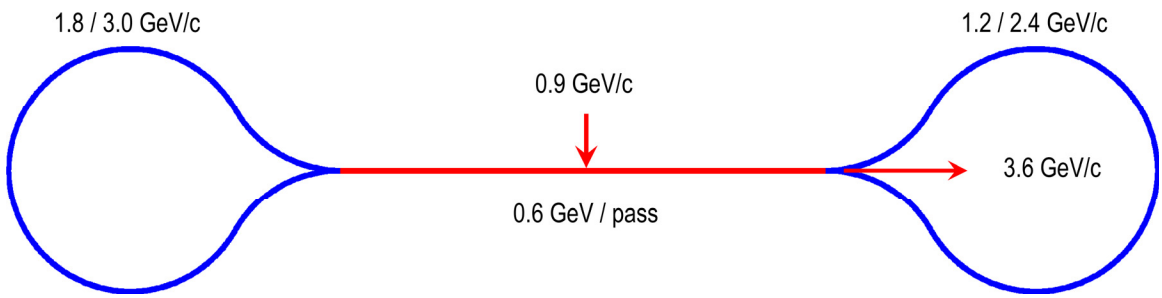

Figure 1: Schematic layout of a 4.5-pass 3.6 GeV/c muon RLA.

* Supported in part by US DOE STTR Grant DE-FG02-08ER86351.

morozov@jlab.org

Linear Optics

We earlier developed a linear optics solution for a multi-pass arc [2-4] based on the conventional linear NS-FFAG lattice [5]. The disadvantage of such a conventional FFAG approach is an inefficient usage of the channel's length due to the alternating outward-inward-outward bends in the underlying triplet structure. In other words, bending the beam by a certain net angle requires a total bend of three times that angle. That made the multi-pass arc very long and hard to compete with the separate arc solution. In the design presented in this paper, we deviate from the conventional FFAG scheme by not requiring regular alternating bends.

A solution satisfying the requirements discussed in the section above can be obtained using only same-direction bends, which can shorten the arc by almost a factor of 3. However, in our parameter range of relatively low energies and large momentum ratio such a solution would still not be optimal in terms of the channel length and magnet parameters. The number of magnets required to meet all of the requirements would make the channel unnecessarily long. Therefore, we introduce another innovation to increase the number of available parameters without increasing the number of magnets. We make the bending angle of each combined function magnet variable with a constraint that the bending angles of all magnets in a super cell must add up to the required fixed total bend. Such a solution combines compactness of the design with all the advantages of our earlier linear NS-FFAG solution [4], namely, large dynamic aperture and momentum acceptance essential for large-emittance muon beams, no need for a complicated compensation of non-linear effects, simpler combined-function magnet design with only dipole and quadrupole field components, etc.

To study the optics for large momentum offsets, we used the Polymorphic Tracking Code (PTC) module of MAD-X [6]. While perturbative method codes are not suitable for such a study, PTC allows symplectic integration through all elements with user control over the precision with full or expanded Hamiltonian.

We assume that the arc is composed of identical super cells. In our energy range, we use the maximum possible bend of 60° per super cell to have the largest possible number of magnets in the super cell and therefore the largest number of free parameters for optics tuning. The super cell consists of 24 combined function magnets with dipole and quadrupole field components. The magnets are 0.5 m long and are separated by 0.2 m gaps. The total arc length is 117.6 m.

Due to the arc's geometric closing, the first and the last few magnets of the arc overlap. These magnets cannot contain quadrupole field components because the symmetry would otherwise lead to the quadrupole fields having opposite slopes in the overlapping magnets. Therefore, we keep the first two magnets of each super cell as pure dipoles. Their bending angles are fixed and are chosen to provide a sufficient separation of the incoming and outgoing higher-momentum beam while keeping the separation of the lower and higher-momentum beams within acceptable limits. Also based on these considerations, we choose the higher 2.4 GeV/c momentum as the reference momentum going through the magnet centers. The beam trajectories at the beginning of the arc are shown in Fig. 2.

The super cell is symmetric with respect to its center. Therefore, out of the 24 magnets constituting the super cell, 12 are independent. As discussed above, 2 of these magnets are pure dipoles with a fixed bending angle of 6° each. The remaining 10 magnets each have variable dipole and quadrupole field components with a constraint that the bending angles of all super cell's magnets add up to a net bend of 60°. This gives a total of 19 independent parameters.

When solving for the periodic orbit and the periodic Twiss functions of the super cell, the initial values of the orbit offset, dispersion, their slopes and the alpha functions were all set to zero at both momenta. The initial values of the horizontal and vertical beta functions were set to 2 m at both momenta to provide easy matching to the linac and to keep the peak values of the beta functions inside the super cell at an acceptable level. The 19 independent parameters discussed above were then adjusted to give zero slopes of the orbit offset, dispersion and beta functions at the center of the super cell at the two momenta. The super cell's symmetry then ensures the appropriate properties at the super cell's exit. Since the 2.4 GeV/c beam goes through the magnet centers, its periodic orbit by definition has zero offset everywhere. This results in a total of 7 constraints. The extra free parameters were used to control the maximum values of the orbit deviation, beta functions and dispersion. In terms of magnetic field requirements, the maximum needed dipole field is about 1.7 T while the maximum quadrupole gradient is about 28 T/m. Figures 3 and 4 show solutions for the periodic orbit, dispersion, and beta functions of the outward-bending super cell at 1.2 and 2.4 GeV/c, respectively. An inward-bending super cell is identical to the outward-bending cell except that its bends are reversed.

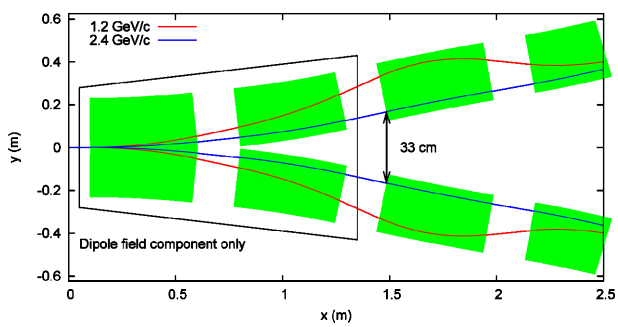

Figure 2: Beginning of the arc with the pure dipoles acting as a spreader/ recombiner of the different momenta trajectories.

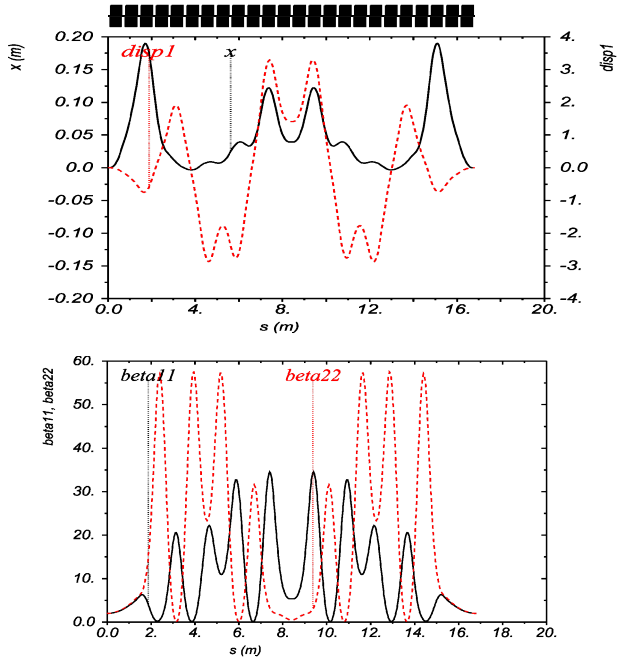

Figure 3: 1.2 GeV/c periodic orbit, dispersion (top) and beta functions (bottom) of the outward bending super cell.

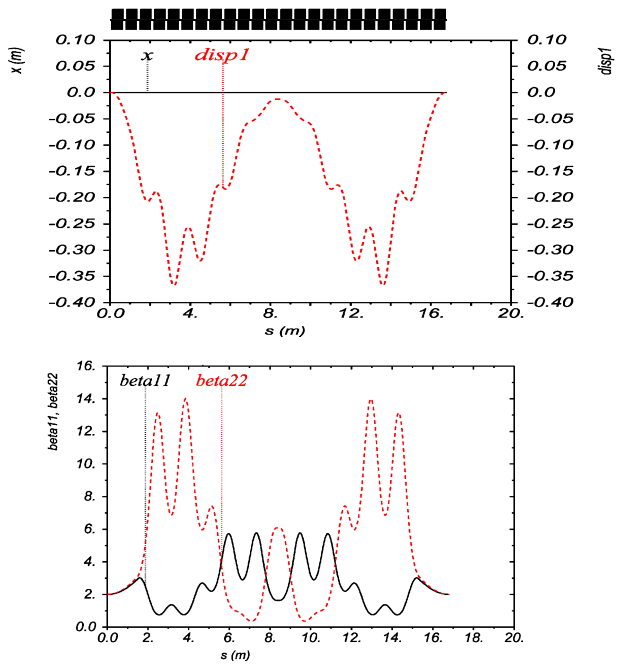

Figure 4: 2.4 GeV/c periodic orbit, dispersion (top) and beta functions (bottom) of the outward bending super cell.

Figure 5 shows geometric layouts of the 1.2 and 2.4 GeV/c closed periodic orbits. The displacement of the 1.2 GeV/c orbit was enhanced by a factor of 10. Note that because of the varying bending angles, the arc is not perfectly circular. The largest orbit separation occurs only in a small number of magnets and is caused by the necessity to spread/recombine the different momenta orbits at the beginning of the arc. The maximum orbit deviation is reduced for smaller momentum ratios such as that of the 1.8/3.0 GeV/c arc.

At few-GeV energies muons are not ultra-relativistic; there is a non-negligible difference in the speeds of 1.2 and 2.4 GeV/c muons. Because of the short arc circumference it was not possible to compensate the time of flight difference by adjusting the path lengths. One can attain an appropriate synchronization with the linac by placing a path-length chicane in front of the arc. Such a chicane would have a cumulative effect on the opposite-direction passes.

We are currently studying the dynamic aperture and momentum acceptance of the arc. Earlier studies with a similar linear lattice yielded promising results [4]. We will investigate chromatic effects and if necessary, implement their control and compensation. Another important aspect that requires investigation is the design sensitivity to magnet misalignments and magnetic field errors. Establishing tolerance levels on these errors is crucial for the costing of large aperture magnets.

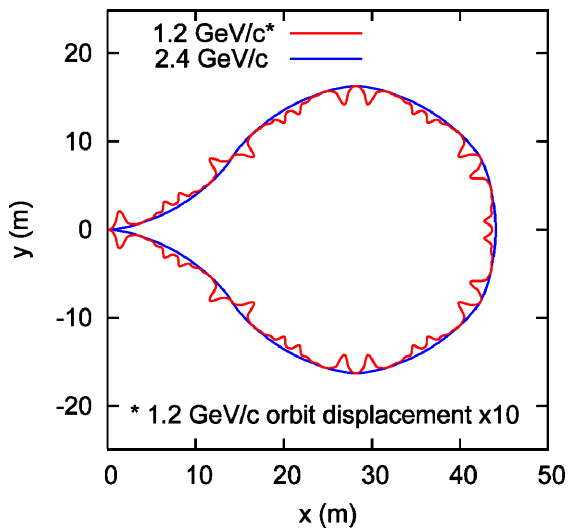

Figure 5: Horizontal (top) and vertical (bottom) maximum-amplitude stable phase-space trajectories for the linear and non-linear NS-FFAG designs.

REFERENCES

[1] S.A. Bogacz et al., "Pulsed-focusing recirculating linacs for muon acceleration", in Proc. PAC'09, Vancouver, BC, Canada.
[2] G.M. Wang et al., "Multipass arc lattice design for recirculating linac muon accelerators", in Proc. PAC'09, Vancouver, BC, Canada.
[3] V.S. Morozov et al., "Muon acceleration with RLA and non-scaling FFAG arcs", in Proc. IPAC'10, Kyoto, Japan.
[4] V.S. Morozov et al., "Matched optics of muon RLA and non-scaling FFAG arcs", in Proc. PAC'11, New York, NY, USA.
[5] D. Trbojevic et al., PRST-AB 8, 050101 (2005).
[6] MAD-X, http://mad.web.cern.ch/mad/

RECENT PROGRESS TOWARD A MUON RECIRCULATING LINEAR ACCELERATOR*

S. A. Bogacz, V. S. Morozov, Y. R. Roblin, Thomas Jefferson National Accelerator Facility, Newport News, VA, USA
K. B. Beard, Muons, Inc., Batavia, IL, USA
A. Kurup, M. Aslaninejad, C. Bonţoiu, J. K. Pozimski
Imperial College of Science and Technology, Department of Physics, London, United Kingdom

Abstract

Both Neutrino Factories (NF) and Muon Colliders (MC) require very rapid acceleration due to the short lifetime of muons. After a capture and bunching section, a linac raises the energy to about 900 MeV, and is followed by one or more Recirculating Linear Accelerators (RLA), possibly followed by a Rapid Cycling Synchnotron (RCS) or Fixed-Field Alternating Gradient (FFAG) ring. A RLA reuses the expensive RF linac section for a number of passes at the price of having to deal with different energies within the same linac. Various techniques including pulsed focusing quadruopoles, beta frequency beating, and multipass arcs have been investigated via simulations to improve the performance and reduce the cost of such RLAs.

BACKGROUND

A neutrino factory and muon collider share many of the same challenges; both must generate pions, then collect muons of both signs from pion decay at relatively low energy, then very quickly accelerate them before the muons all decay. Their acceleration schemes are not quite identical, as the emittance of the beams may not be the same, but most of the features discussed here are applicable to both.

A Recirculating Linear Accelerator (RLA) passes particles through the same linac multiple times. To maintain a sufficient focusing on subsequent passes, we investigated using rapidly ramped quadruopoles [2], but found that for this application beta frequency beating [3] alone was a sufficient solution.

INTERNATIONAL DESIGN STUDY

The International Design Study for the Neutrino Factory (IDS-NF) baseline design involves a complex chain of accelerators including a single-pass prelinac, two recirculating linacs (RLA) and a fixed field alternating gradient accelerator (FFAG).[1] As part of the study, our group simulated the muon acceleration from 0.2 to 12.6 GeV using OptiM [4], Elegant [5] and G4beamline [6] in the prelinac and RLAs.

The baseline design will evolve in light of recent measurements, but the current design was basis for this work.

* Funding: Supported in part by US DOE STTR Grant DE-FG02-08ER86351. Notice: Authored by Jefferson Science Associates, LLC under U.S. DOE Contract No. DE-AC05-06OR23177.

Prelinac

The first linac follows the capture and bunching section and accelerates muons of both signs from about 244 to 900 MeV [7][8] total energy. It must accept a high emittance beam about 30 cm wide with a 10% energy spread.[9] This linac uses counterwound, shielded superconducting solenoids and 201 MHz superconducting cavities. The prelinac uses two types of cryomodules, both with a bore radius of 23 cm. The first is 3m long with a single RF cell, while the second is 5m long with a double RF cell.

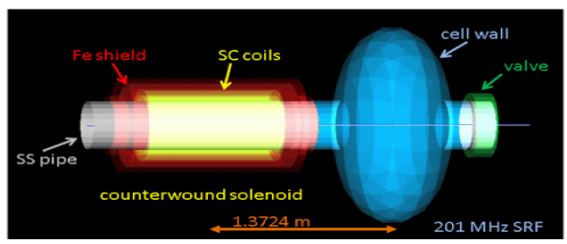

Figure 1a: G4beamline model of a 3m prelinac cryomodule.

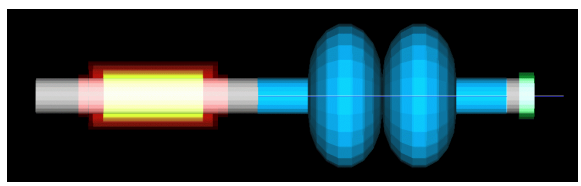

Figure 1b: G4beamline model of a 5m prelinac cryomodule.

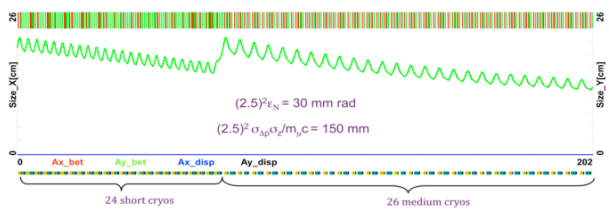

Figure 1c: OptiM model of the prelinac.

Chicane

The current chicane separates the $\mu^{\pm}$ with a dipole, then each is directed down 1.75m into the plane of RLA I, then directed by dipoles into the middle of the linac. On

subsequent passes, the injection dipole separates the returning $\mu^{\pm}$, so a mini-chicane in the linac is used to correct the paths.

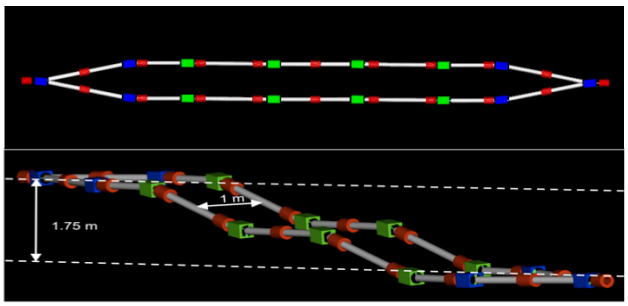

Figure 2a: G4beamline model of the prelinac to RLA I chicane.

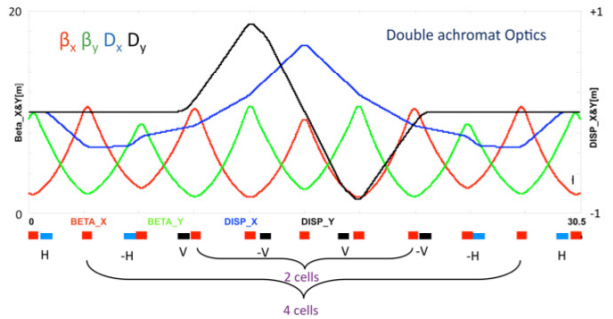

Figure 2b: OptiM model of the prelinac to RLA I chicane.

The current version of the chicane was found to interfere mechanically with the cryomodules and is being redesigned.

RLA I

RLA I is a 4½ pass 0.6 GeV/pass RLA which takes the beam from 0.9 to 3.6 GeV. To preserve the symmetry for the beta beating technique, the beam is injected into the middle of the linac. The strength of the quadrupoles is set with their gradients decreasing roughly linearly with distance from the middle of the linac. The beta functions then oscillate, but remain reasonable at the entrances to the arcs.

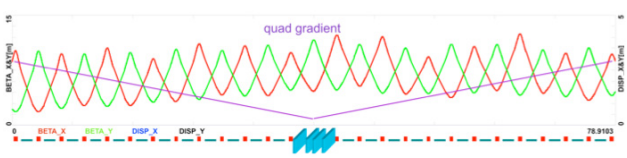

Figure 3a. Increasing quadrupole strength with distance to center of linac and 1st whole pass beta functions.

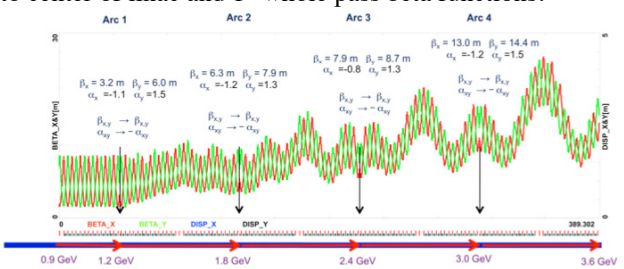

Figure 3b. Beta beating in the RLA I linac for all passes.

There are 2 teardrop-shaped arcs at either end of the linac; each arc is matched to the beta function at that exit of the linac for its pass. Muons of opposite sign travel in the same direction through the linac and in opposite directions around the arcs. To avoid interference, dipoles lift the plane of the lower energy arc by 1m. The beam in then extracted at the end of the linac.

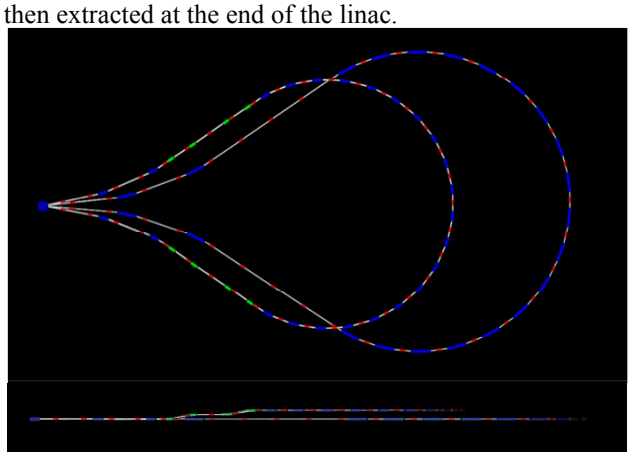

Figure 4a: Top and side views of a G4beamline model of the RLA I arcs#1 (1.2 GeV) and #3 (2.4 GeV).

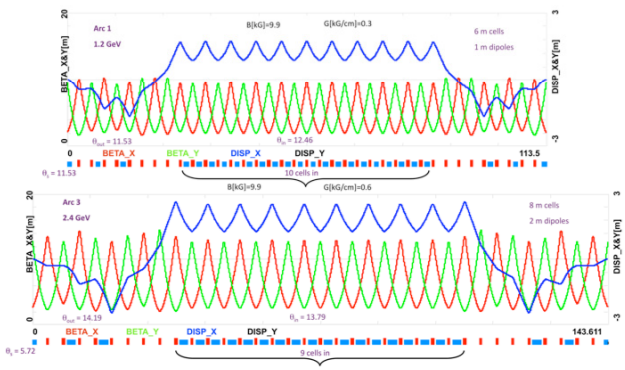

Figure 4b: OptiM model of RLA I arc #1 and #3.

Each switchyard only accommodates only 2 momenta.

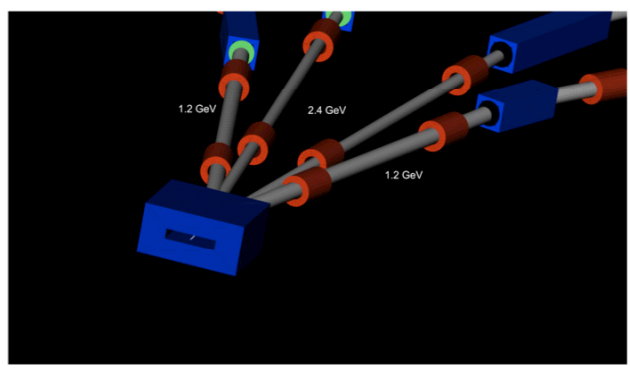

Figure 5. G4beamline model of RLA I switchyard for arc#1 and #3.

RLA II

RLA I is followed by very similar, but larger, 4½ pass 2 GeV/pass RLA II that takes the beam from 3.6 to 12.6 GeV.

ISBN 978-3-95450-115-1
1423

Table 1: RLA I and II Properties

	RLA I	L_{cell}	L_{dipole}	RLA II	L_{cell}	L_{dipole}
	GeV	m	m	GeV	m	m
enter	0.9			3.6		
linac	0.6	6.0		2.0	12.0	
arc1	1.2	6.0	1.0	4.6	12.0	2.0
arc2	1.8	7.0	1.5	6.6	14.0	3.0
arc3	2.4	8.0	2.0	8.6	16.0	4.0
arc4	3.2	9.0	2.5	10.6	18.0	5.0
exit	3.6			12.6		

MULTIPASS ARCS

If two arcs could be replaced by a single arc that could transport two very different momentum beams, the RLA could be greatly simplified by eliminating the one arc's chicanes and the most of the switchyard.

While the concept of a multipass arc is described in detail elsewhere [10], a brief description is given here. The arc is built of cells, and those cells are constructed of linear combined-functions magnets with variable dipole and quadrupole field components. Those components and magnet orientations are adjusted to control the optics of the multiple passes. Unlike a fixed field alternating gradient design, opposing bends are not required.

The cells are set such that the dispersion and displacement is zero at the end of each cell and the beta functions are the same and match that of the linac for each pass. A prototype system using multipass arcs is being considered [11].

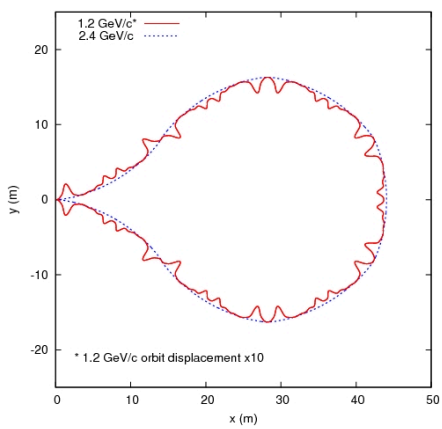

Figure 6. Multipass arc with orbits.

FUTURE WORK

Very recent results have significantly altered the requirements for a neutrino factory.[12] The final energy is now expected to be 10 GeV, so the RLAs would directly feed the decay ring, eliminating the need for a synchrotron to follow the RLAs. This will require a re-optimization of both the current prelinac and RLA designs.

REFERENCES

[1] Interim Design Report, IDS-NF-020, http://www.ids-nf.org
[2] S. A. Bogacz et al., IPAC'10, Kyoto, Japan, May 2010, pp 3602-3604.
[3] S. A. Bogacz, NuFact'09, Chicago, USA, July 2009, pp 363-367.
[4] V. Lebedev, OptiM - http://wwwbdnew.fnal.gov/pbar/organizationalchart/lebedev/OptiM/optim.htm
[5] M. Borland, Elegant - http://www.aps.anl.gov/Accelerator_Systems_Division/Operations_Analysis/oagPackages.shtml
[6] T. J. Roberts, G4beamline - http://g4beamline.muonsinc.com
[7] C. Bontoiu et al., IPAC'10, Kyoto, Japan, May 2010, pp 4590-4592.
[8] J. S. Berg et al., Phys. Rev. ST Accel. Beams, 9:011001, 2006.
[9] S. A. Bogacz. Nucl. Phys. B Proc. Suppl., 149:309–312, 2005.
[10] V. S. Morozov, et al., in Proc. IPAC'11, San Sebastion, Spain, March 2011, pp 868.
[11] S. A. Bogacz, et al., "Scaled Electron Model of a Dogbone Muon RLA with Multi-pass Arcs", MOPPC045, this conference.
[12] K. Long, IDS-NF Plenary Meeting, April 2012, Glasgow, UK.

SCALED ELECTRON MODEL OF A DOGBONE MUON RLA WITH MULTI-PASS ARCS *

S.A. Bogacz#, A.M. Hutton, G.A. Krafft, V.S. Morozov, Y.R. Roblin, Jefferson Lab, Newport News, VA, USA
K.B. Beard, R.P. Johnson Muons, Inc., Batavia, IL, USA

Abstract

The design of a dogbone Recirculated Linear Accelerator, RLA, with linear-field multi-pass arcs was earlier developed [1] for accelerating muons in a Neutrino Factory and a Muon Collider. It allows for efficient use of expensive RF while the multi-pass arc design based on linear combined-function magnets exhibits a number of advantages over separate-arc or pulsed-arc designs. Such an RLA may have applications going beyond muon acceleration. This paper describes a possible straightforward test of this concept by scaling a GeV scale muon design for electrons. Scaling muon momenta by the muon-to-electron mass ratio leads to a scheme, in which a 4.5 MeV electron beam is injected at the middle of a 3 MeV/pass linac with two double-pass return arcs and is accelerated to 18 MeV in 4.5 passes. All spatial dimensions including the orbit distortion are scaled by a factor of 7.5, which arises from scaling the 200 MHz muon RF to the frequency readily available at CEBAF: 1.5 GHz. The footprint of a complete RLA fits in an area of 25 by 7 m. The scheme utilizes only fixed magnetic fields including injection and extraction. The hardware requirements are not very demanding, making it straightforward to implement.

MUON RLA WITH TWO-PASS ARCS

A schematic layout of a dogbone-shaped muon RLA, proposed for future Neutrino Factory [2] is illustrated in the top portion of Fig. 1. Reusing the same linac for multiple (4.5) beam passes provides for a more compact accelerator design and leads to significant cost savings. In the conventional scheme with separate return arcs [3], different energy beams coming out of the linac are separated and directed into appropriate arcs for recirculation. Therefore, each pass through the linac would require a separate fixed-energy arc, increasing the complexity of the RLA. We propose a novel return-arc optics design based on linear combined function magnets with variable dipole and quadrupole field components, which allows two consecutive passes with very different energies to be transported through the same string of magnets [4].

* Supported in part by US DOE STTR Grant DE-FG02-08ER86351.

bogacz@jlab.org

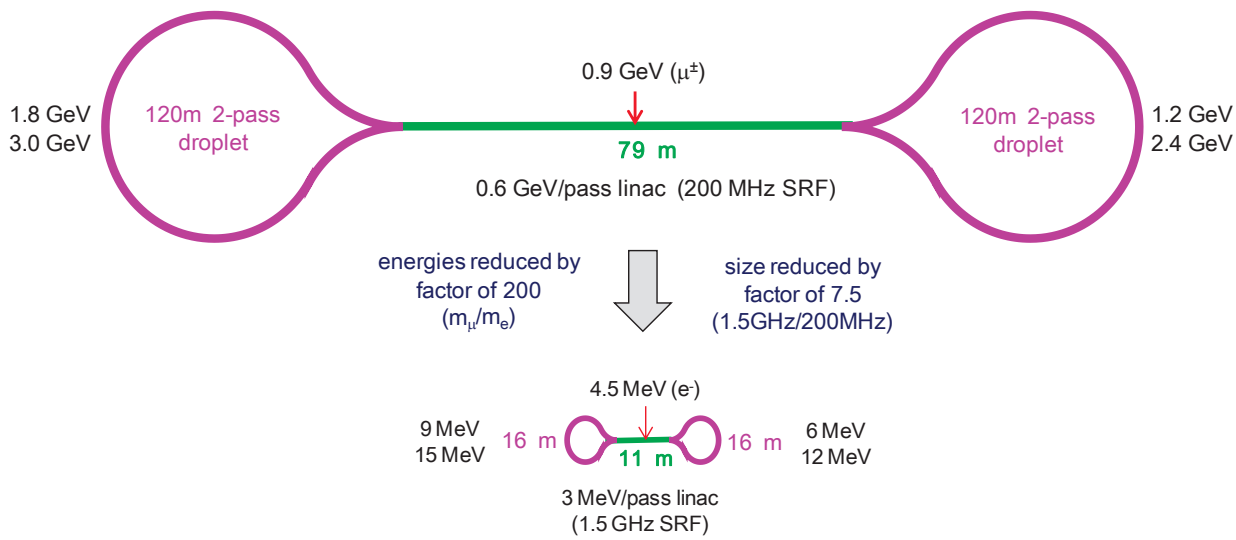

Figure 1: Schematic layout of a GeV-scale muon RLA with two-pass return arcs. A path to an 'electron model' is outlined: scaling 3.6 GeV muon RLA to 18 MeV model and replacing 200 MHz RF with a 1.5 GHz CEBAF cavity.

ISBN 978-3-95450-115-1

SCALED DOWN ELECTRON MODEL

Here, we propose a straightforward test of this concept by scaling the above GeV-scale muon RLA design for electrons. Scaling muon momenta by the muon-to-electron mass ratio (~ 200) yields a scheme, in which a 4.5 MeV electron beam is injected into the middle of a 3 MeV/pass linac with two double-pass return arcs and then is accelerated to 18 MeV in 4.5 passes.

The second scaling, would involve replacing the original low frequency (200 MHz) RF, required to accommodate inherently long muon bunches, with readily available high frequency CEBAF RF (1.5 GHz). All spatial dimensions including the orbit distortion would then scale down by the ratio of the two frequencies (factor of 7.5). As a consequence, the scaled down electron model would fit in a modest test cave of 25 by 7 meters.

For the remainder of this paper, we will describe the principle of multi-pass arc architecture, a possible magnet design and field requirements, as well as a complete conceptual RLA design.

MULTI-PASS ARC OPTICS

Design Concept

The droplet arc design consists of super cells, which are required to satisfy the following basic conditions at two discrete energies (6 and 12 MeV):

- Each super cell exhibits periodic solutions for the orbit and the Twiss functions.
- At the beginning and at the end of each super cell, the periodic orbit offset, dispersion and their slopes are all zero.

The first condition ensures that the super cells bending in the same direction are optically matched while the second one provides optical matching of the cells bending in the opposite directions. The second condition also implies that the beam is centered in the linac and that the linac is dispersion free.

Linear Optics

Optics solution satisfying the above conditions can be obtained using only same-direction bends, which significantly shortens the arc (by almost a factor of 3) compared to the conventional linear NS-FFAG lattice [5], which involves alternating the 'outward-inward-outward' bends in the underlying triplet structure. We make the bending angle of each combined function magnet variable with a constraint that the bending angles of all magnets in a super cell must add up to the required fixed total bend. Such a solution combines compactness of the design with all the advantages of a linear NS-FFAG [6], namely, large dynamic aperture and momentum acceptance essential for large-emittance muon beams, no need for a complicated compensation of non-linear effects, simpler combined-function magnet design with only dipole and quadrupole field components. We use the maximum possible bend of 60° per super cell to accommodate the largest possible number of magnets in the super cell and therefore to have the largest number of free parameters for optics tuning. The extra free parameters were used to control the maximum values of the orbit deviation, beta functions and dispersion. Figure 2 shows solutions for the periodic orbit and dispersion of the outward-bending super cell at 6 and 12 MeV/c, respectively. An inward-bending super cell is identical to the outward-bending cell except that its bends are reversed. The super cell consists of 24 combined function magnets with dipole and quadrupole field components. The magnets are 6.5 cm long and are separated by 3 cm gaps. The total arc length is 16 m. In terms of magnetic field requirements, the maximum needed dipole field is about 650 Gauss while the maximum quadrupole gradient is about 850 Gauss/cm.

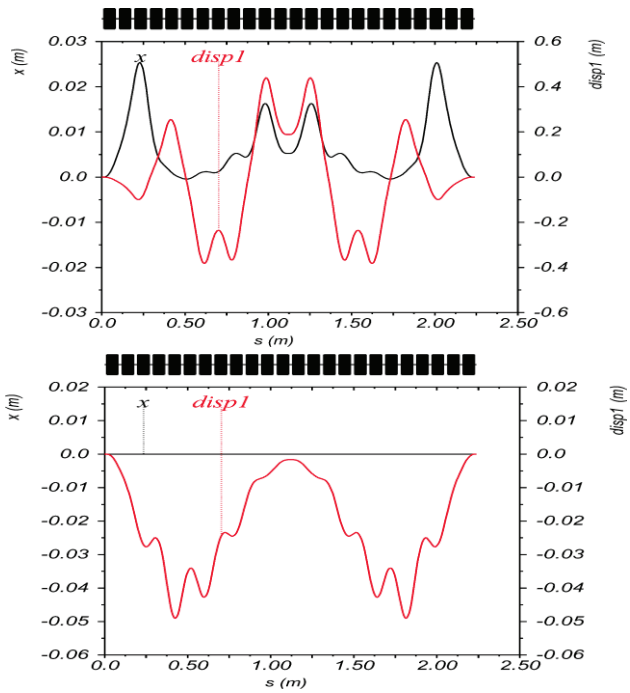

Figure 2: 6 MeV (top) and 12 MeV (bottom) periodic orbits and dispersions of the outward bending super cell.

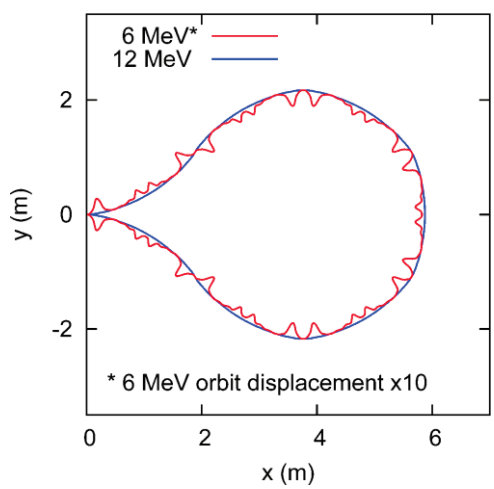

Figure 3: Layout of the 6 and 12 MeV reference orbits.

Fig. 3 illustrates geometric layouts of the 6 and 12 MeV closed periodic orbits. Note that because of the varying bending angles, the arc is not perfectly circular. The largest orbit separation occurs only in a small number of magnets and is caused by the necessity to spread/recombine the different momenta orbits at the beginning of the arc.

ARC TO MULTI-PASS LINAC MATCHING

As a proof-of-principle, one can design a multi-pass linac with energy gain of 3 MeV per pass, which is matched by-design to previously described two-pass arcs for both passes simultaneously. As described in [3] the above multi-pass linac optics can be accomplished by appropriately 'tailored' focusing profile along the linac - the strengths of individual linac's fixed-field quadrupoles. Here, they are treated as free parameters used to control the beta functions at linacs ends for all consecutive passes. The proof-of-principle solution [4] was designed by modifying the so-called bi-sected linac profile [3], where the quadrupole strengths increase linearly (in a mirror-symmetric fashion) from the linac's center toward the ends.

MAGNET DESIGN AND FIELD QUALITY

Design Choice

Each of 7 super-periods required to complete the droplet arc is configured with 24 individual combined function magnets: 6.5 cm in length and with 5 cm of the horizontal aperture. These magnets will be mounted on a rectangular vacuum chamber; 2.3 meter long and shaped into a 60^0 arc. As for the magnet design, a combined function Panofsky quadrupole with integral dipole windings, similar to Jlab's FEL design [7], provides a very attractive solution for an independent electrical control of both the magnetic field and its gradient.

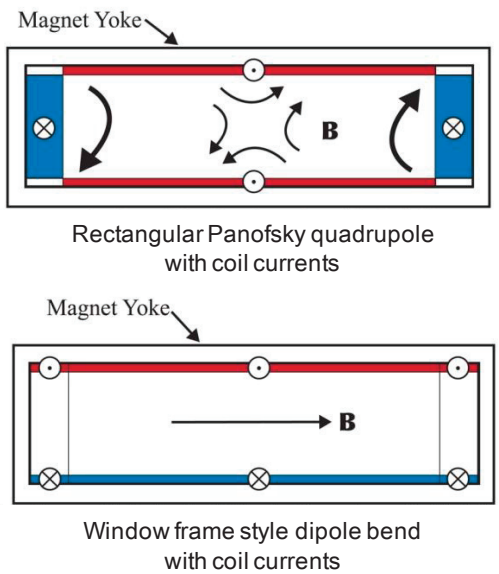

Figure 4: Quadrupole and Dipole Current Flows [7].

Relatively weak magnets, satisfying our strength requirements, can be built 'flattened' with no compromise to their field gradient uniformity and have a window frame-like yoke that, at full quadrupole current, is not near saturation [7]. Superposition of a dipole onto the Panofsky quad adds current to one of the four coils and subtracts it from its opposing coil. This is accomplished by adding variable current coils to the vacant corners of the original Panofsky design as illustrated in Fig. 4.

Field Quality Requirements – Error Sensitivity

The two-pass arc optics, illustrated in Fig. 2, was checked for error sensitivity. We launched a mini Monte Carlo simulation by creating 25 virtual arc lattices with statistically distributed magnet mis-alignment (200 μm, rms, displacement error) as well as magnet mis-powering (with 10^{-4} relative field error, rms) for both the dipole and quadrulpole components. Using pairs of horizontal and vertical correctors placed after each magnet the resulting orbit deviation was steered back to to the design orbit within 20 μm level, which corresponds to the accuracy of the orbit measurement (BPM accuracy).

CONCLUSIONS

We propose a straightforward test of a GeV scale muon RLA by scaling the muon design for electrons (via the muon-to-electron mass ratio). Presented 'electron model' features: a 4.5 MeV electron beam injected at the middle of a 3 MeV/pass linac with two double-pass return arcs, The beam is accelerated to 18 MeV in 4.5 passes. All spatial dimensions of the full scale RLA are shortened by a factor of 7.5, as a consequence of using a readily available 1.5 GHz CEBAF cavity, rather than the original 200 MHz RF. The footprint of a complete RLA 'demo' fits in an area of 25 by 7 m. The scheme utilizes only fixed magnetic fields including injection and extraction. Engineering design and fabrication of linear-field combined-function magnets does not seem to present a challenge [7].

REFERENCES

[1] S.A. Bogacz, Nucl. Phys. B Proc. Suppl., **149**, p. 309, 2005.
[2] Design Report, IDS-NF-020, http://www.ids-nf.org
[3] S.A. Bogacz et al., "Recirculating linear accelerators for future muon facilities" IPAC'10, Kyoto, p. 3602.
[4] V.S. Morozov et al., "Multi-pass muon RLA return arcs based on linear combined-function", in Proc. IPAC'11, San Sebastian, p. 2784.
[5] G.M. Wang et al., "Multipass arc lattice design for recirculating linac muon accelerators", in Proc. PAC'09, Vancouver, BC, p. 2736.
[6] V.S. Morozov et al., "Matched optics of muon RLA and non-scaling FFAG arcs", in Proc. PAC'11, New York, NY, p. 163.
[7] G.H. Biallas et al., "Combined Panofsky Quadrupole & Corrector Dipole" in Proc. PAC'07, Albuquerque, NM, p. 602.

ISBN 978-3-95450-115-1

Linear fixed-field multipass arcs for recirculating linear accelerators

V. S. Morozov,[1] S. A. Bogacz,[1] Y. R. Roblin,[1] and K. B. Beard[2]
[1]*Thomas Jefferson National Accelerator Facility, Newport News, Virginia 23606, USA*
[2]*Muons, Inc., Batavia, Illinois 60510, USA*
(Received 6 April 2012; published 14 June 2012)

Recirculating linear accelerators (RLA's) provide a compact and efficient way of accelerating particle beams to medium and high energies by reusing the same linac for multiple passes. In the conventional scheme, after each pass, the different energy beams coming out of the linac are separated and directed into appropriate arcs for recirculation, with each pass requiring a separate fixed-energy arc. In this paper we present a concept of an RLA return arc based on linear combined-function magnets, in which two and potentially more consecutive passes with very different energies are transported through the same string of magnets. By adjusting the dipole and quadrupole components of the constituting linear combined-function magnets, the arc is designed to be achromatic and to have zero initial and final reference orbit offsets for all transported beam energies. We demonstrate the concept by developing a design for a droplet-shaped return arc for a dogbone RLA capable of transporting two beam passes with momenta different by a factor of 2. We present the results of tracking simulations of the two passes and lay out the path to end-to-end design and simulation of a complete dogbone RLA.

DOI: 10.1103/PhysRevSTAB.15.060101 PACS numbers: 29.20.Ej, 29.27.Eg, 41.75.−i, 41.85.Ja

I. INTRODUCTION

Reusing the same linac in a recirculating linear accelerator (RLA) [1] for multiple beam passes provides for a more compact accelerator design and leads to significant cost savings. In a conventional RLA [2], the different-energy passes coming out of the linac are separated and directed into individual return arcs for recirculation. Thus, each pass through the linac requires a separate fixed-energy arc, increasing the complexity of the RLA. The maximum number of passes through the RLA's linac is often limited by design considerations for the switch-yard, which first spreads the different-energy passes to go into the appropriate arcs and then recombines them to align the beam with the linac axis. In this paper, we present a return-arc design concept, which allows two and potentially more consecutive passes with very different energies to be transported through the same string of magnets. In the proposed design, the arc is built of linear combined-functions magnets with variable dipole and quadrupole field components, which are adjusted to control the optics of the multiple passes.

The multipass arc design has a number of advantages over separate-arc [2] or pulsed-arc [3] approaches. It eliminates the need for a complicated switch-yard, it reduces the total beam-line length, there is no need to accommodate multiple beam lines in the same tunnel or construct separate tunnels for individual arcs, and there is no need for vertical bypasses, which may be required for separate arcs complicating the optics. This helps to increase the number of passes through the linac thus enhancing the top energy available with the same-size footprint. The design employs only fixed-field magnets, which alleviates the requirements on magnets and power supplies and greatly simplifies injection and extraction. The fixed-field design also allows for a rapid continuous-wave (CW) acceleration. Another important feature of the design is a large dynamic aperture characteristic of linear-field lattices. It is fairly straightforward and inexpensive to design and build linear-field combined-function magnets even with relatively large apertures [4].

A dogbone-shaped RLA [5] with multipass arcs [6] was initially proposed for accelerating muons in the future Neutrino Factory and Muon Collider. Of all available particle species, accelerating a muon beam is, perhaps, the most challenging due to its large 6D emittance, short muon lifetime, and the wish to accelerate both muon charges in the same RLA simultaneously. Therefore, in this paper, we will be paying special attention to muon acceleration aspects. However, the multipass arc design concept is also applicable to both dogbone and racetrack RLA's for electrons and ions. Besides high-energy physics, such RLA's can find uses in free electron lasers and as accelerators for nuclear physics. Compact smaller-scale RLA's can benefit numerous applications [7–10] in industry, material science, astrophysics, medical isotope production, radiation cancer therapy, power generation, homeland security, and many other areas.

II. DESIGN REQUIREMENTS

Our goal is to configure the arc's magnetic structure so that it can accommodate multiple beam passes with substantially different energies. Keeping the emphasis on

muon beams, the following constraints are imposed on the arc design.

(a) The arc's magnetic optics must be mirror symmetric for each pass, so that the beams of both charges can propagate through the arc in opposite directions equivalently. For a symmetric magnetic structure, this leads to the linear optics requirement that, for all passes, the Twiss β functions must be equal and have equal-magnitude opposite-sign slopes (as a function of the longitudinal coordinate) at the beginning and end of the arc:

$$\beta^i_{x,y\,B} = \beta^i_{x,y\,E}, \tag{1}$$

$$\alpha^i_{x,y\,B} = -\alpha^i_{x,y\,E}, \tag{2}$$

where $\beta_{x,y}$ and $\alpha_{x,y}$ are the horizontal and vertical Twiss β and α functions, respectively, subscripts B and E denote the locations at the beginning and end of the arc, and superscript i refers to the pass number.

(b) Assuming a flat horizontal arc, each pass's reference orbit must have zero horizontal offset x and zero slope x' (the prime denotes a derivative with respect to the longitudinal coordinate) at the beginning and end of the arc:

$$x^i_B = x^i_E = 0, \tag{3}$$

$$x'^i_B = x'^i_E = 0, \tag{4}$$

to ensure that all energy beams are centered inside the linac.

(c) The horizontal dispersion D_x and its slope D'_x must be zero at the beginning and end of the arc for all passes:

$$D^i_{x\,B} = D^i_{x\,E} = 0, \tag{5}$$

$$D'^i_{x\,B} = D'^i_{x\,E} = 0, \tag{6}$$

to keep the linac dispersion free.

(d) The times of flight or, equivalently, the path lengths of the different-energy passes must provide proper synchronization with the linac.

(e) The orbit offsets as well as beta functions and dispersion must be maintained within reasonable limits for all energies to keep the magnet aperture sizes acceptable.

(f) The dynamic aperture and momentum acceptance at all energies must be adequate for large-emittance beams such as those of muons.

Since the arc's magnetic structure is mirror symmetric, if one chooses some values of $\beta^i_{x,y\,B}$ and $\alpha^i_{x,y\,B}$ and sets $x^i_B = 0$, $x'^i_B = 0$, $D^i_{x\,B} = 0$, and $D'^i_{x\,B} = 0$, it is sufficient to require that, at the arc's symmetry point,

$$\alpha^i_{x,y\,S} = 0, \tag{7}$$

$$x'^i_S = 0, \tag{8}$$

$$D'^i_{x\,S} = 0, \tag{9}$$

where subscript S denotes the symmetry point location in the middle of the arc. The conditions given by Eqs. (7)–(9) impose a total of $4 \times i$ constraints. These constraints are optimal from the point of view of matching to the linac, however, they are not necessary requirements. We are intentionally considering a conservative case with the most constraints to illustrate the multipass arc concept. Depending on a specific situation, one might also consider relieving some of the constraints.

It is often convenient, especially for large arcs, to construct the lattice of identical superperiods. One must then apply the constraints of Eqs. (7)–(9) to each superperiod, i.e., indices B, E, and S now refer to the beginning, end, and symmetry point, respectively, of the superperiod. In addition, to ensure proper matching between the superperiods, one must set $\alpha^i_{x,y\,B} = 0$. This is equivalent to requiring that each superperiod has a periodic optics solution at each energy. Another advantage of this approach is that, under the discussed constraints, superperiods bending in opposite directions but otherwise identical are automatically matched to each other. This allows, for instance, construction of droplet-shaped return arcs, which include outward- and inward-bending sections. Reversing all bends in a superperiod preserves the linear optics but reflects the signs of x and D_x. Given the constraints of Eqs. (3), (5), and (6), the opposite-bending periods are then still matched to each other.

Note that the points between the superperiods are convenient locations for insertion of any additional straight sections if needed because the dispersion there is suppressed for all passes and all-energy beams are centered in the beam line as per Eqs. (3), (5), and (6). Therefore, only β function matching is required. Inserting same-length straight sections between all superperiods also preserves the arc's overall geometry.

III. DESIGN APPROACH

We first considered an arc design based on a nonlinear nonscaling fixed-field alternating-gradient (NS-FFAG) lattice [11]. The underlying structure was a triplet composed of in-out-in-(out-in-out-)bending combined-function magnets with fixed dipole and variable quadrupole, sextupole, and octupole field components. Having a few multipole components in each magnet provides a large number of knobs to satisfy conditions (7)–(9). An appropriate optics solution was demonstrated [6,12]; however, optimization of the nonlinear dynamics for multiple passes is rather challenging.

Therefore, we next investigated a linear NS-FFAG arc design. The lattice structure was similar to that of the nonlinear solution but each combined-function magnet only had fixed dipole and variable quadrupole field components. A solution based on the linear NS-FFAG approach was also demonstrated [13]. It had a number of advantages over the nonlinear design: (i) much greater dynamic aperture characteristic of linear-field lattices; (ii) simpler optimization of

the nonlinear dynamics; (iii) simpler control of the reference orbit at each energy because of a lower sensitivity to magnetic field parameters than in the nonlinear case, which makes it easier to minimize the orbit excursion and adjust the path-length/time-of-flight; (iv) simpler control over the β functions and dispersion; (v) lower sensitivity to magnetic field errors and magnet misalignments and simpler error correction; (vi) simpler combined-function magnet design with dipole and quadrupole field components only.

Since each combined-function magnet now only had one variable parameter, namely, the quadrupole strength, the number of magnets had to be increased to provide enough knobs to meet all of the constraints in Eqs. (7)–(9). Furthermore, because of the mirror symmetry, only one-half of the magnets in a superperiod are independent. This made each superperiod longer and/or more finely structured. Another disadvantage shared by both the nonlinear and linear NS-FFAG-based designs is an inefficient use of the channel's length due to the alternating in-out-in (or out-in-out) bends in the underlying triplet structure, i.e., bending the beam by a certain net angle requires a total bend of 3 times that angle. This makes the NS-FFAG-based designs relatively long and hard to compete with the separate-arc arrangement. In the concept presented in this paper, we deviate from the conventional FFAG scheme by not requiring regular alternating bends.

A solution satisfying the requirements discussed in Sec. II can be obtained using only same-direction bends, which would shorten the arc by almost a factor of 3. However, there is still the problem of the large number of linear combined-function magnets required to satisfy Eqs. (7)–(9). Therefore, we introduce another concept [14] doubling the number of available parameters without increasing the number of magnets. We make the bending angles of some of the combined-function magnets variable with a constraint that the bending angles of all magnets in a superperiod must add up to a given fixed total bend:

$$\sum_n \theta_n = \theta_{\text{net}} = \text{const}, \tag{10}$$

where θ_n is the bending angle of nth magnet in the superperiod defined for a nominal-energy trajectory going along the center of the magnet and θ_{net} is the superperiod's total bending angle. Note that the superperiod's magnetic structure is maintained mirror symmetric, therefore, only a half of the magnets in the superperiod can have independent field parameters, namely, the bending angles and quadrupole strengths. Such an approach combines compactness of the design with all of the above advantages of a linear NS-FFAG scheme.

IV. LINEAR OPTICS

We demonstrate the multipass arc concept in application to a proposed dogbone-shaped muon RLA [5] with two double-pass droplet return arcs. In that scheme illustrated in Fig. 1, both positively and negatively charged 0.9 GeV/c muon beams are injected in the middle of a 0.6 GeV/pass linac. The linac is then traversed by the beams 4 times accelerating them to 3.6 GeV/c. Therefore, one of the return arcs must accommodate 1.2 and 2.4 GeV/c muon momenta, while the other arc must accommodate 1.8 and 3.0 GeV/c momenta. Since the two arcs can be designed using the same approach, below we focus our discussion on the 1.2/2.4 GeV/c arc whose design is somewhat more challenging due to the greater fractional momentum difference of the two passes.

Each droplet arc consists of a 60° outward bend, a 300° inward bend, and another 60° outward bend so that the net bend is 180°. This arc geometry has the advantage that, if the outward and inward bends are composed of similar cells, the geometry automatically closes without the need for any additional straight sections, making it simpler and more compact.

To study the optics for large momentum offsets, we used the polymorphic tracking code (PTC) module [15] of MAD-X [16]. While perturbative-method codes are not suitable for such studies, PTC allows symplectic integration through all elements with user control over the precision with full or expanded Hamiltonian.

We assume that the arc is composed of identical superperiods. In our relatively low energy range, we use the maximum possible bend of 60° per superperiod to have the largest possible number of magnets in the superperiod and, therefore, the largest number of free parameters for optics tuning. The superperiod consists of 24 combined-function magnets with dipole and quadrupole field components. For this initial demonstration, we chose hard-edge sector magnets because it is more straightforward to subdivide them into thin slices for tracking. The magnets are 0.5 m long and are separated by 0.2 m gaps. The total arclength is then 117.6 m. Note that, in practice, it is more convenient to use

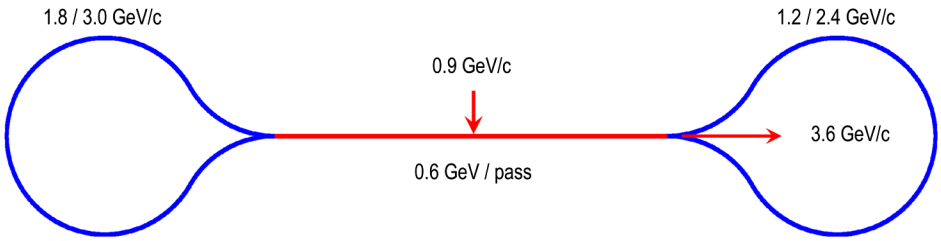

FIG. 1. Schematic layout of a 4.5-pass 3.6 GeV/c muon RLA.

rectangular magnets and there is no conceptual problem with converting the magnet shape in the solution from sector to rectangular. It is also straightforward to modify the design to include realistic magnet fringe fields.

Because of the droplet arc's geometric closing, the first and last few magnets of the arc overlap. These magnets cannot contain quadrupole field components because the symmetry would otherwise lead to the quadrupole fields having opposite slopes in the overlapping magnets. Therefore, we keep the first two magnets of each superperiod as pure dipoles. Their bending angles are fixed and are chosen to provide a sufficient separation of the incoming and outgoing higher-momentum beam while keeping the separation of the lower- and higher-momentum beams within acceptable limits. Also based on these considerations, we choose the higher 2.4 GeV/c momentum as the reference momentum going through the magnet centers.

The beam trajectories at the beginning of the arc are shown in Fig. 2. After the first two magnets, the distance of about 33 cm between the incoming and outgoing 2.4 GeV/c orbits is perhaps enough to insert separate magnets in the incoming and outgoing lines. For simplicity and to illustrate our multipass concept more clearly, the design presented in this paper is composed of identical symmetric supercells, which means that there are pure dipoles at the beginning and end of each supercell. However, none of the arc's inner magnets have to be pure dipoles. This opens another avenue for design optimization, in particular, one can reduce the orbit excursion and therefore the required magnet apertures inside the arc.

Note that a racetrack geometry does not have the above pure-dipole spreader/recombiner restriction, i.e., all magnets in a racetrack arc can have both dipole and quadrupole field components, which can help minimize the orbit excursion everywhere in the arc. Additionally, neither geometry requires that one of the passes has to go through the magnet centers. A solution can be obtained when momenta of all passes are different from the nominal center-line momentum [13]. This might be particularly useful for adjusting the path-lengths/times-of-flight of the different passes for synchronization with the linac.

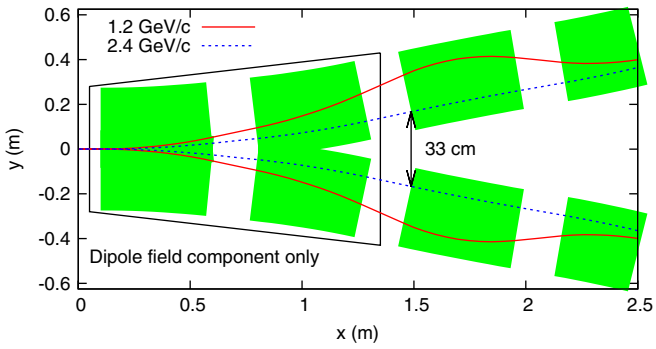

FIG. 2. The apex of the droplet arc with the pure dipoles acting as a spreader/recombiner of the different-momentum trajectories.

As discussed in Sec. II, each superperiod is symmetric with respect to its center. Therefore, out of the 24 magnets constituting the superperiod, 12 are independent. The first two of these magnets are pure dipoles with fixed bending angles of 6° each. The remaining 10 magnets each have variable dipole and quadrupole field components with a constraint of Eq. (10) on the bending angles that the superperiod's net bend is 60°. This gives a total of 19 independent parameters.

Following the description in Sec. II, when solving for the 1.2 and 2.4 GeV/c reference orbits and optics of the superperiod, the beginning values of the orbit offset (x^i_B), dispersion ($D^i_{x\,B}$), their slopes (x'^i_B and $D'^i_{x\,B}$), and the α functions ($\alpha^i_{x,y\,B}$) were all set to zero for both momenta. The initial values of the horizontal and vertical β functions ($\beta^i_{x,y\,B}$) were all set at 2 m for both momenta to provide easy matching to the linac and to keep the peak values of the β functions in the superperiod at acceptable levels. The 19 independent magnet parameters discussed above were then tuned to meet the requirements of Eqs. (7)–(9), i.e., to give zero slopes of the orbit offset, dispersion, and β functions at the center of the superperiod for the two momenta. The symmetry then ensures that Eqs. (3)–(6) are satisfied at the superperiod's exit.

Since the 2.4 GeV/c beam goes through the magnet centers, its reference orbit by definition has zero offset everywhere. This results in a total of 2 passes × 4 constraints/pass − 1 = 7 constraints with 19 fitting parameters available. The extra free parameters were used to control the maximum values of the orbit deviation, β functions, and dispersion. The resulting magnet parameters in the first half of the outward-bending superperiod are listed in Table I. In terms of magnetic field requirements, the maximum dipole field in Table I is about 1.7 T while the maximum quadrupole gradient is about 28 T/m.

TABLE I. Bending angles θ, bending radii ρ, dipole fields B, and quadrupole strengths $\partial B_y/\partial x$ of the magnets in the first half of the outward-bending superperiod. The parameters are defined with respect to the channel's nominal axis coinciding with the 2.4 GeV/c reference orbit.

Magnet #	θ (°)	ρ (m)	B (T)	$\partial B_y/\partial x$ (T/m)
1	−6.000	4.775	−1.677	0.000
2	−6.000	4.775	−1.677	0.000
3	1.976	14.497	0.552	19.529
4	−5.008	5.720	−1.399	−24.584
5	−2.823	10.149	−0.789	28.342
6	−2.572	11.140	−0.719	−22.321
7	0.501	57.222	0.140	21.206
8	−1.950	14.691	−0.545	−21.230
9	−1.763	16.245	−0.493	23.233
10	−2.472	11.588	−0.691	−27.653
11	−1.982	14.456	−0.554	24.536
12	−1.907	15.023	−0.533	−18.612

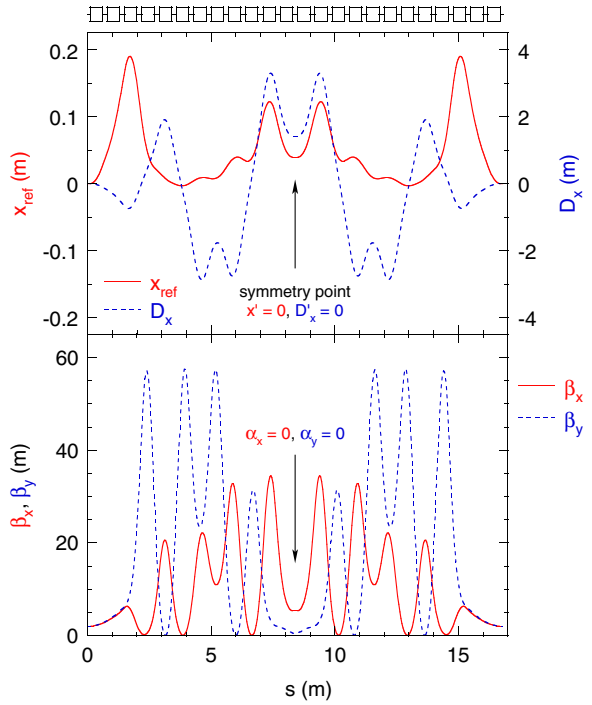

FIG. 3. 1.2 GeV/c optics of an outward-bending superperiod: the horizontal reference orbit x_{ref} and dispersion D_x (top) and the horizontal and vertical β functions (bottom).

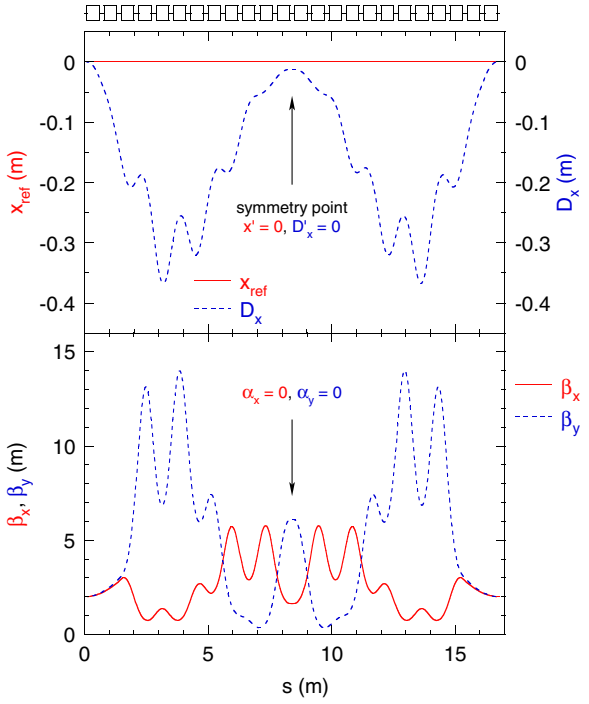

FIG. 4. 2.4 GeV/c optics of an outward-bending superperiod: the horizontal reference orbit x_{ref} and dispersion D_x (top) and the horizontal and vertical β functions (bottom).

Figures 3 and 4 show 1.2 and 2.4 GeV/c solutions, respectively, for the periodic orbits, dispersion, and β functions of an outward-bending superperiod. Since the only difference of an inward-bending superperiod from the outward-bending one is that its bends are reversed, its optics is identical to Figs. 3 and 4 except that the signs of the reference orbits and dispersion are flipped. The 1.2 GeV/c optics of a complete droplet arc is shown in Fig. 5. It illustrates how the whole arc is built out of individual outward- and inward-bending superperiods.

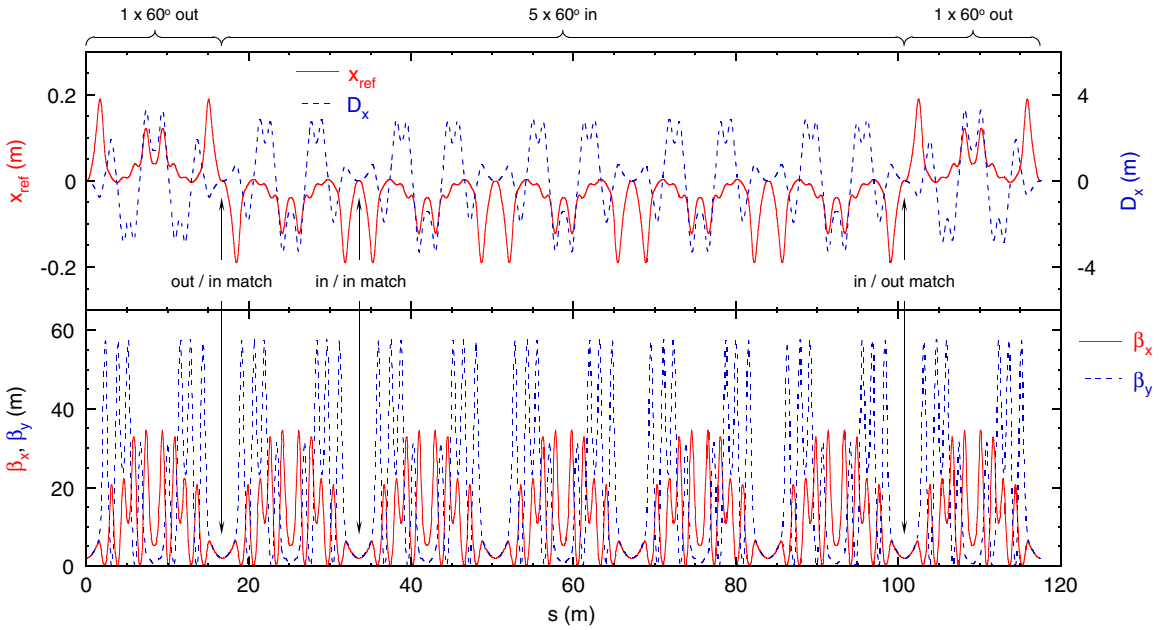

FIG. 5. 1.2 GeV/c optics of a complete droplet arc: the horizontal reference orbit x_{ref} and dispersion D_x (top) and the horizontal and vertical β functions (bottom). The arrows point to the different-type junctions between the outward- and inward-bending superperiods.

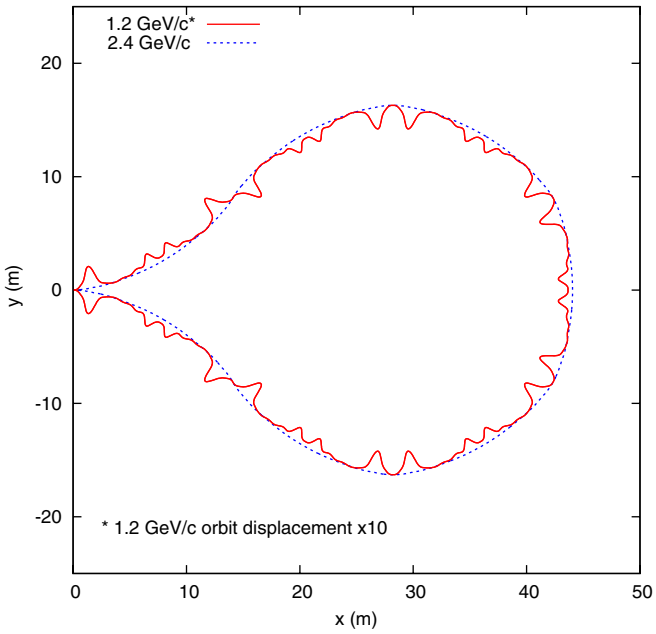

FIG. 6. Geometric layout of the 1.2 and 2.4 GeV/c reference orbits. The displacement of the 1.2 GeV/c orbit is magnified by a factor of 10.

Note, in particular, the matching points between the superperiods bending in the same and opposite directions. The 2.4 GeV/c optics of a complete arcs can be constructed similarly using the data in Fig. 4.

Figure 6 shows geometric layout of the 1.2 and 2.4 GeV/c reference orbits. The displacement of the 1.2 GeV/c orbit was enhanced by a factor of 10. Note that because of the varying bending angles, the arc is not perfectly circular. The largest orbit separation of about 19 cm is determined primarily by the necessity to spread/recombine the different-momentum orbits at the beginning of the arc. It sets the requirements on the magnet apertures. However, such a large separation occurs only in a small number of magnets while the remaining magnets may have smaller apertures. The maximum orbit deviation is reduced for smaller momentum ratios such as that of the 1.8/3.0 GeV/c arc.

The magnet parameters in Table I and the orbit offsets in Figs. 3–5 are specified with respect to a nominal-momentum trajectory, which defines the nominal axis of the magnetic channel. As discussed above, the nominal momentum in our case was set at 2.4 GeV/c. In practice, however, the actual magnets do not have to be centered on the channel's nominal axis. In fact, to optimally use the magnets' good-field regions and minimize the required apertures, the center of each physical magnet transversely should be placed approximately halfway between the 1.2 and 2.4 GeV/c orbits. Linearity of the magnetic field allows for a straightforward transformation of the dipole component (the quadrupole component is unchanged) to account for the transverse shift.

V. TRACKING RESULTS

To validate our linear optics design, we used the PTC module of MAD-X to track a bunch of 3000 muons through the droplet arc. The tracking results for the 1.2 and 2.4 GeV/c passes are shown in Figs. 7 and 8 respectively. In each case, the initial bunch distribution was Gaussian with no cross correlations between the 6D phase-space coordinates. At each momentum, the horizontal ε_{xN} and vertical ε_{yN} normalized rms emittances were both 30 mm mrad, the rms bunch length σ_z was 1 cm, and the rms relative momentum spread $\Delta p/p$ was 1×10^{-3}.

Figures 7 and 8 compare the horizontal (a), vertical (b), and longitudinal (c) phase-space distributions of the initial bunch (shown in blue) to those after the bunch's single pass through the complete droplet arc (shown in red). We intentionally chose the values of the initial transverse and longitudinal emittances at the levels where the bunch was beginning to get deformed at 1.2 GeV/c to probe the limits of the arc's dynamic aperture and momentum acceptance. Note, in particular, in Fig. 7(c) that the longitudinal dynamics starts getting affected by the amplitude path-length dependence, which is a general problem of large-transverse-emittance beams [17]. The particle transmission rates (not including muon decay) were 92.8% at 1.2 GeV/c and 100% at 2.4 GeV/c.

The results shown in Figs. 7 and 8 indicate that, even without any nonlinear optimization, the arc's dynamic aperture might be adequate for deeply cooled muon beams [18,19]. To accommodate a large momentum spread characteristic of muon beams, the arc's longitudinal dynamics

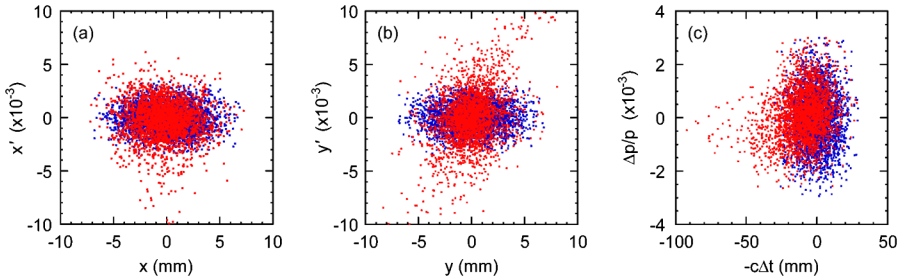

FIG. 7. Horizontal (a), vertical (b), and longitudinal (c) phase-space distributions of a 1.2 GeV/c muon bunch before (blue) and after (red) passing through the droplet arc.

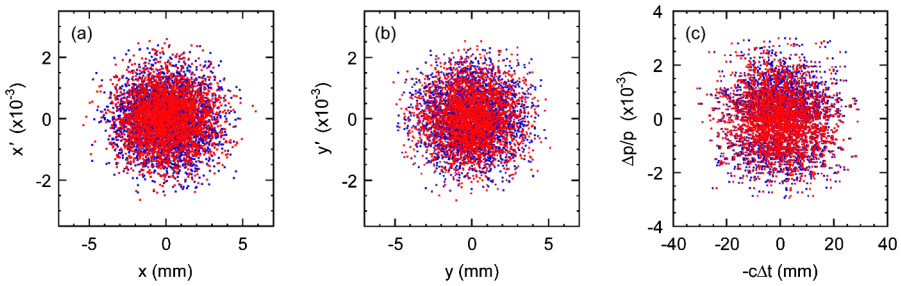

FIG. 8. Horizontal (a), vertical (b), and longitudinal (c) phase-space distributions of a 2.4 GeV/c muon bunch before (blue) and after (red) passing through the droplet arc.

needs to be optimized by compensating chromatic and amplitude-dependent path-length effects and preparing a proper initial bunch state. On the other hand, even without any optimization, the arc properties readily meet the dynamic aperture and momentum acceptance requirements for the typical accelerator beam emittances of most other particle species, such as electrons, protons, deuterons, etc. The tracking in Figs. 7 and 8 was performed for an ideal lattice with no magnet misalignments or magnetic field errors. Studying the sensitivity to such imperfections is not one of the goals of this paper; however, preliminary simulations of these effects seem rather encouraging.

VI. MATCHING TO LINAC AND COMPLETE RLA DESIGN CONSIDERATIONS

A complete end-to-end RLA design is beyond the scope of this paper. However, as a proof of principle, one can design a corresponding linac with energy gain of 600 MeV per pass, which is matched by design to previously described two-pass arcs for both passes simultaneously. As illustrated in Fig. 9, this multipass linac optics can be accomplished by adjusting the strengths of the linac's fixed-field quadrupoles. The presented solution was accomplished by modifying the so-called bisected linac profile [20], where the quadrupole strengths increase linearly from the linac's center toward the edges. Perhaps the Twiss parameters at the entrance into the arcs can be further optimized from the point of view of better matching to the linac; optimizing the arc and linac optics is an iterative process.

Another critical issue that needs to be considered when developing a complete RLA design is proper synchronization of all passes with the linac's rf. The difference in the times of flight of the different passes in each arc must be either close to zero or close to an integer number of rf oscillation periods. The time-of-flight difference between the passes arises due to a combination of the differences in their speeds and path lengths.

Since 1.2 and 2.4 GeV/c muons are not ultrarelativistic, there is a non-negligible effect of their speed difference. As it can be seen from Fig. 6, the 1.2 GeV/c orbit in our design is clearly longer than the 2.4 GeV/c one. Thus, the time-of-flight difference between the two passes must be adjusted to the nearest integer number (including zero) of rf periods. One option is to manipulate the path lengths inside the arc. For instance, one can make 1.2 GeV/c to be the central momentum instead of 2.4 GeV/c in the arc's inner superperiods, which would compensate some of the time-of-flight difference. Another option is to place

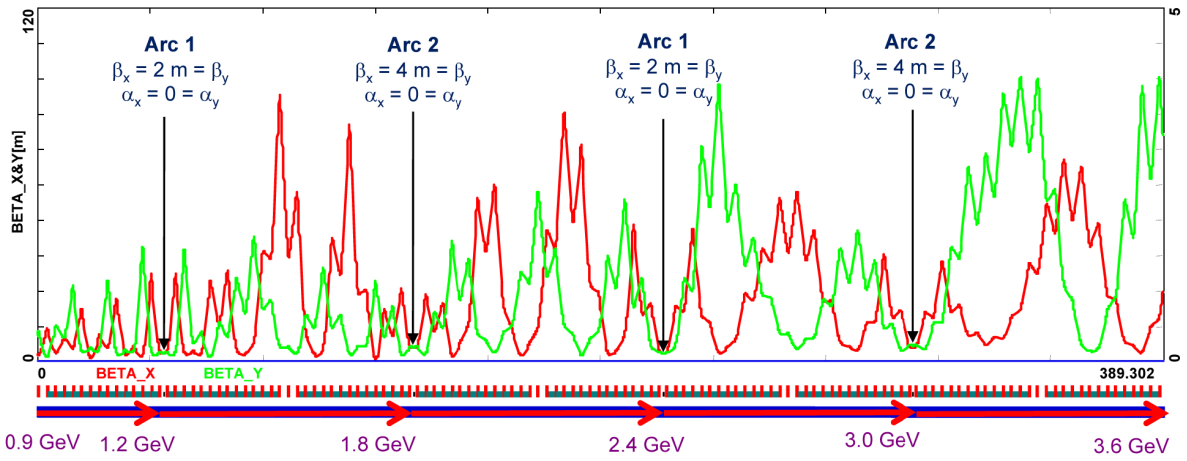

FIG. 9. Linac optics matched to both arcs for all passes simultaneously. The arrows indicate arc locations.

path-length chicanes [21,22] between the superperiods or in front of the arc. A chicane located in front of the arc would have a cumulative effect on the opposite-direction passes. Combining both options might be the best approach.

VII. CONCLUSIONS

We developed a concept of an RLA return arc based on linear combined-function magnets, in which two and potentially more consecutive passes with very different energies are transported through the same string of magnets. We demonstrated that, by adjusting the dipole and quadrupole field components of the constituting linear combined-function magnets, the arc can be made achromatic and to have zero initial and final reference orbit offsets for two beam energies. Such an approach combines compactness of the design with the many benefits [13,14] of a conventional linear NS-FFAG scheme.

We applied the concept to design a droplet-shaped return arc for a dogbone muon RLA capable of transporting two beam passes with momenta different by a factor of 2. We obtained solutions for the reference orbits and linear optics of the two passes. Tracking simulations of the developed design showed that, with appropriate optimization of the longitudinal dynamics, it may be adequate for deeply cooled muon beams and it readily meets the dynamic aperture and momentum acceptance requirements for the typical accelerator beam emittances of most other particle species. There is a straightforward path to a complete RLA design. In that regard, we showed a proof-of-principle transverse matching of the arc to the linac for all passes simultaneously and discussed synchronization of the different passes with the linac's rf.

The proposed multipass arc concept has a number of attractive features. It can increase the number of passes through the linac, thus, leading to a more efficient use of rf and higher energies available with the same-size accelerator footprint. It eliminates the need for a complicated switch-yard, it reduces the total beam-line length, there is no need to accommodate multiple beam lines in the same tunnel or construct separate tunnels for individual arcs. The design relies solely on fixed magnetic fields, thus, weakening the requirements on magnets and power supplies and greatly simplifying injection and extraction. It allows for a CW operation. Engineering design and fabrication of linear-field combined-function magnets does not seem to present a challenge [4] even for relatively large apertures. Thus, the multipass approach may benefit many applications in science and industry.

ACKNOWLEDGMENTS

This manuscript has been authored by Jefferson Science Associates, LLC under Contract No. DE-AC05-06OR23177 with the U.S. Department of Energy. This work was supported in part by the U.S. Department of Energy Small Business Technology Transfer Grant No. DE-FG02-08ER86351. We are grateful to A. M. Hutton, R. P. Johnson, G. A. Krafft, and D. Trbojevic for their help and advice.

[1] R. E. Rand, *Recirculating Electron Accelerators* (Harwood Academic Publishers, New York, 1984).
[2] C. W. Leemann, D. R. Douglas, and G. A. Krafft, Annu. Rev. Nucl. Part. Sci. **51**, 413 (2001).
[3] K. B. Beard, R. P. Johnson, S. A. Bogacz, and G. M. Wang, in *Proceedings of the 23rd Particle Accelerator Conference, Vancouver, Canada, 2009* (IEEE, Piscataway, NJ, 2009), WE6PFP097, p. 2733.
[4] G. H. Biallas, N. Belcher, D. Douglas, T. Hiatt, and K. Jordan, in *Proceedings of the 2007 Particle Accelerator Conference, Albuquerque, New Mexico* (IEEE, New York, 2007), MOPAS074, p. 602.
[5] S. A. Bogacz, G. Wang, and R. P. Johnson, in Proceedings of the 23rd Particle Accelerator Conference, Vancouver, Canada, 2009 (Ref. [3]), WE6PFP100, p. 2742.
[6] G. M. Wang, R. P. Johnson, S. A Bogacz, and D. Trbojevic, in Proceedings of the 23rd Particle Accelerator Conference, Vancouver, Canada, 2009 (Ref. [3]), WE6PFP098, p. 2736.
[7] Accelerators for America's Future, DOE Report, June 2010 [http://www.acceleratorsamerica.org/files/Report.pdf].
[8] S. S. Kurennoy, A. J. Jason, and H. Miyadera, in *Proceedings of the International Particle Accelerator Conference, Kyoto, Japan* (ICR, Kyoto, 2010), WEPE075, p. 3518.
[9] R. W. Hamm and M. E. Hamm, Phys. Today **64**, 46 (2011).
[10] CAARI 2012: 22nd International Conference on the Application of Accelerators in Research and Industry, Fort Worth, TX [http://www.caari.com/].
[11] D. Trbojevic, E. D. Courant, and M. Blaskiewicz, Phys. Rev. ST Accel. Beams **8**, 050101 (2005).
[12] V. S. Morozov, S. A. Bogacz, and D. Trbojevic, in Proceedings of the International Particle Accelerator Conference, Kyoto, Japan (Ref. [8]), WEPE084, p. 3539.
[13] V. S. Morozov, S. A. Bogacz, Y. R. Roblin, K. B. Beard, and D. Trbojevic, in *Proceedings of the 2011 Particle Accelerator Conference, NY, USA* (IEEE, New York, 2011), MOP052, p. 196.
[14] V. S. Morozov, S. A. Bogacz, Y. R. Roblin, and K. B. Beard, in *Proceedings of the 2nd International Particle Accelerator Conference, San Sebastian, Spain, 2011* (EPS-AG, San Sebastian, Spain, 2011), MOPZ031, p. 868.
[15] E. Forest, F. Schmidt, and E. McIntosh, CERN Report No. CERN-SL-2002-044 (AP) (2002); KEK Report No. 2002-3 (2002) [http://cern.ch/Frank.Schmidt/report/sl-2002-044.pdf].
[16] http://cern.ch/madx.
[17] J. S. Berg, Nucl. Instrum. Methods Phys. Res., Sect. A **570**, 15 (2007).
[18] Ya. S. Derbenev and R. P. Johnson, in *Proceedings COOL'05*, AIP Conf. Proc. No. 821 (AIP, Melville, NY, 2006), p. 420.

[19] V. S. Morozov, Ya. S. Derbenev, A. Afanasev, R. P. Johnson, B. Erdelyi, and J. A. Maloney, in Proceedings of the 2nd International Particle Accelerator Conference, San Sebastian, Spain, 2011 (Ref. [14]), WEPZ009, p. 2784.

[20] S. A. Bogacz, in *Proceedings NuFact'09*, AIP Conf. Proc. No. 1222 (AIP, Melville, NY, 2010), p. 363.

[21] H. A. Enge, Rev. Sci. Instrum. **34**, 385 (1963).

[22] H. L. Owen and P. H. Williams, Nucl. Instrum. Methods Phys. Res., Sect. A **662**, 12 (2012).